

*Citation for published version:*

Papatzani, S, Badogiannis, E & Paine, K 2018, 'The pozzolanic properties of inorganic and organomodified nano-montmorillonite dispersions', *Construction and Building Materials*, vol. 167, pp. 299-316.  
<https://doi.org/10.1016/j.conbuildmat.2018.01.123>

*DOI:*

[10.1016/j.conbuildmat.2018.01.123](https://doi.org/10.1016/j.conbuildmat.2018.01.123)

*Publication date:*

2018

*Document Version*

Peer reviewed version

[Link to publication](#)

*Publisher Rights*

CC BY-NC-ND

**University of Bath**

**Alternative formats**

If you require this document in an alternative format, please contact:  
[openaccess@bath.ac.uk](mailto:openaccess@bath.ac.uk)

**General rights**

Copyright and moral rights for the publications made accessible in the public portal are retained by the authors and/or other copyright owners and it is a condition of accessing publications that users recognise and abide by the legal requirements associated with these rights.

**Take down policy**

If you believe that this document breaches copyright please contact us providing details, and we will remove access to the work immediately and investigate your claim.

# **The pozzolanic properties of inorganic and organomodified nano-montmorillonite dispersions**

Styliani Papatzani<sup>1,2,\*</sup>, Efstratios G. Badogiannis<sup>3</sup> and Kevin Paine<sup>1</sup>

<sup>1</sup>*BRE Centre for Innovative Construction Materials, University of Bath, BA2 7AY, Bath, UK*

<sup>2</sup>*Greek Ministry of Culture, Directorate of Restoration of Medieval and Post-medieval Monuments, Tzireon 8-10, 11742, Athens, Greece, Country*

<sup>3</sup>*Civil Engineering Department, National Technical University of Athens, Athens 15773, Greece*

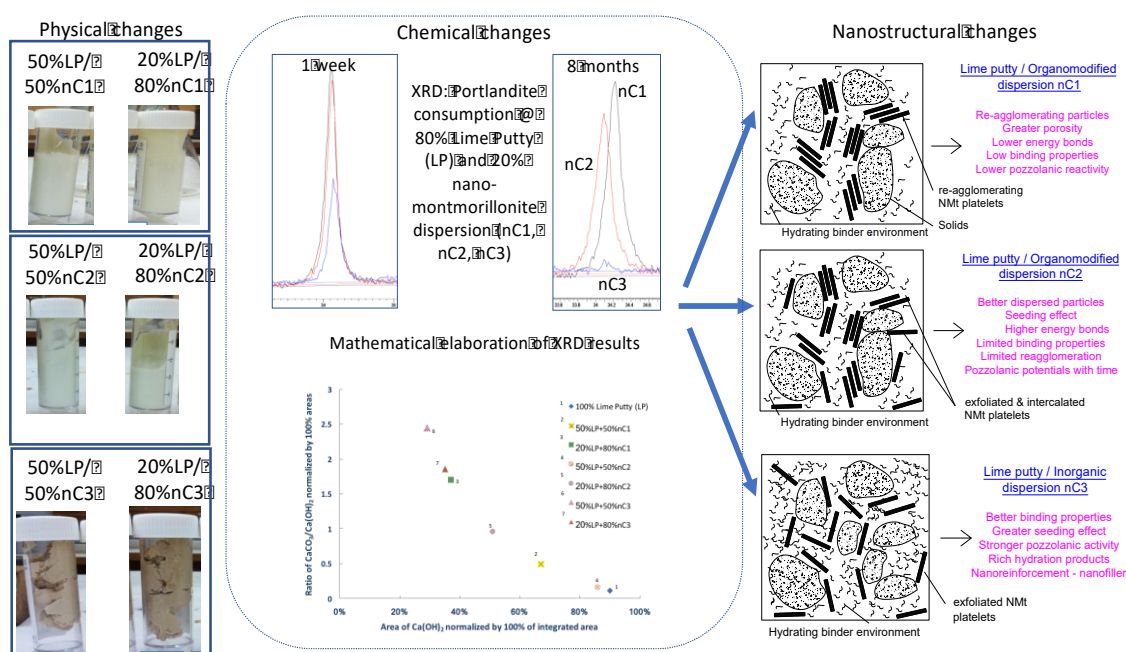
\*Corresponding author: E-mail: spapatzani@gmail.com, Tel +30 6985877730

## **Abstract**

The pozzolanic potentials of three non-thermally treated, nano-montmorillonite (NMt) dispersions were investigated by a new method involving the analysis of NMt/lime putty pastes via TGA/dTG and XRD crystallographic and semi-quantitative analysis. The criterion conceived was validated at eight days and eight months and was additionally verified via the Chapelle method. The inorganic NMt dispersion showed the most pronounced pozzolanic behaviour promoting  $\text{Ca(OH)}_2$  consumption towards calcium

silicate/aluminate hydrates formation and binding behaviour. The two organomodified NMt dispersions exhibited pozzolanicity increasing with time. The results can pave the way for advances in cement science and restoration mortars development for historical structures rehabilitation, where low CO<sub>2</sub>-footprint, natural inorganic materials are a prerequisite.

Keywords: inorganic and organomodified nano-montmorillonite dispersions, lime putty pastes, XRD, TGA/dTG, pozzolanic reactions, Chapelle test, non-calcined



## 1. Introduction

Montmorillonite (Mt) is one of the main minerals found in bentonites, a naturally occurring clay. Mt is rich in stacks of layers/platelets held together by interlayer cations, by van der Waals forces, by electrostatic force or by hydrogen bonding inhibiting the solubility or miscibility [1]. Moreover, Mt is a 2:1 layered silicate, implying that each layer is composed of two silicon tetrahedral sheets bonding with one octahedral sheet of alumina between them. Isomorphous substitution takes place in the octahedral sheet where most hydroxyl groups are located apart from the broken sides of each particle [2]. Surface modifiers, such as quaternary ammonium salts (quats) inserted in the interlayer space can fully separate these platelets (exfoliation or if at a lower extent, intercalation), creating individual nano-thick, plate-like particles. These particles, hereafter referred to as nano-montmorillonite (NMt), can engage in chemical reactions analogous to their specific surface area.

Apart from these organic modifiers, which usually cause platelet separation by cation exchange, and produce a pulverized product, Mt can be exfoliated in water in its pristine condition. In fact, even in earlier research focused on polymer-clay nanocomposites it has been stated that apart from organomodification, small additions of water were adequate for clay exfoliation [3]. Therefore, if Mt is dispersed in water, it can maintain its inorganic nature and platelets can remain dispersed with the help of inorganic surfactants. Inorganic surfactants promote the homogenous dispersion of the NMt platelets in the aqueous environment. NMt platelets dispersed in water are easier to handle compared to those in powder form, because agglomeration of particles into clusters (usually of micron scale or bigger) is avoided. In addition, NMt dispersed in water, provides greater miscibility with other cementing constituents.

The nanoengineering process of Mt layer separation and the NMt products have attracted the attention of cement scientists who seek to use the exfoliated NMt particles as a means of additional nucleation sites or nano-scale reinforcement in the hydrating cement matrix [4]. The nature, nanostructure, production methods, effect of modifiers and dispersants and the configurations of the NMt platelet separation for use as polymer nanocomposites or adsorption materials can be found in the literature [3,5–7]. However, limited research is presented on the use of NMt and this research is applied in cement binder formulations [4,8–10].

Supplementary cementitious materials (SCM) used in lime or cement mortars can be classified as (i) pozzolanic (ii) latent-hydraulic or (iii) fillers. Pozzolanic SCM are the most common. A pozzolanic SCM consists of a material rich in amorphous alumina or silica that is non-reactive with other compounds and water as is to form additional hydration products. However, in the alkaline medium created by the dissolution of calcium hydroxide in water the silicate or aluminosilicate networks break down to form calcium silicate and/or calcium aluminate hydrates. The relative pozzolanicity of a material depends on a high content of amorphous phases and a high specific surface area.

With respect to pozzolanic studies on clays, at present only the pozzolanic activity of thermally and mechanically treated kaolin [2,11,12] or halloysite nanoclay particles [13] has been confirmed. There is disagreement on the pozzolanic potential of Mt with some researchers stating that calcined Mt mineral exhibits limited pozzolanic activity depending on the calcination temperature [2], while others claim that natural and calcined Mt contribute to pozzolanic reactions [14]. That is to say, Mt so far has only been investigated in its calcined form. However, the high temperatures involved for calcinations increase the CO<sub>2</sub> footprint of the material. With the evolution of nanotechnology, which allows us to manipulate matter at levels slightly above the atomic, another option rather than calcination arises; the

nanomodification of Mt, i.e. the breaking of the forces holding its platelets together so that the nanoplatelets will then be individually available for reactions, as explained above. With respect to NMt, the incorporation of Cloisite®30B to waste glass powder cement mortars exhibited enhanced pozzolanic reactivity leading to improved mechanical properties [15]. In another study the incorporation of Cloisite®30B to ordinary Portland cement showed pozzolanic potentials [16]. Still, one element of the process is to nanomodify the Mt and another part is to disperse it in water, so as to render it more compatible with binders, more easily usable with higher potentials for mass production. So far, only the authors' team has presented research on the effect of various NMt dispersions in the hydrating cement paste [4,8–10] and of this work only part of it has proven the pozzolanic potentials of the inorganic NMt dispersion in ternary Portland cement-limestone binders [8]. Therefore, although the pozzolanic contribution of NMt in cement binders has been confirmed, the pozzolanic behaviour of NMt as a raw material is yet to be scrutinized. However, given the complex nature of NMt dispersions, containing not only Mt but also modifiers and dispersing agents, a criterion taking into account the decomposition of various components within the same temperature intervals is yet to be presented. This elaborate research will provide sound calculations of pozzolanicity in more intricate matrices such as those of NMt enhanced cement binders.

The currently widely used pozzolanic additions such as fly ash, are being depleted [17] and others such as silica fume are difficult to handle and increase the total cost of the binder. The abundance of bentonite in nature, from which Mt can be received, and the ease of Mt exfoliation in water in the case of inorganic dispersions [9,10], make NMt a potentially interesting alternative SCM. Furthermore, the reaction of the exfoliated platelets around hydrated Portland cement particles can enable a tortuous microcrack propagation pattern, hence providing nanoreinforcement at the nanolevel to the microlevel, as confirmed by a series of

experiments [10]. Other clays, such as metakaolin, get activated by heating above 700°C, increasing the embodied CO<sub>2</sub> of the binder. Therefore, avoiding calcination and nanomodifying Mt, comprises a way of producing sustainable low carbon additions for the future. Given that the filler effect of Mt is confirmed [2], what remains to be assessed is the pozzolanic effect of NMt dispersions, which are easier to handle than their powder counterparts, however exhibit an inherent difficulty because of the presence of the modifier and surfactant.

The depletion of natural and man-made pozzolanas and the need to lower the carbon dioxide footprint by avoiding pozzolanas produced by calcination, is calling for new materials and methods to be developed. From the above, it can be established that neither the pozzolanic activity of non-calcined NMt nor the pozzolanicity of non-calcined NMt dispersions has been examined previously. Such a discovery could be proven valuable for cement science, because it will allow the use of NMt dispersions, whose main constituent, montmorillonite, is abundant in nature and environmentally friendly, as SCM, avoiding the otherwise added environmental cost of calcination. Therefore, this research programme was designed to investigate the pozzolanic properties of two different aqueous organomodified NMt dispersions and one aqueous inorganic NMt dispersion. Characterization techniques for this standalone methodology of assessing the pozzolanic behaviour only necessitated: thermal gravimetry analysis and differential thermogravimetry (TGA/dTG), X-Ray diffraction (XRD) crystallography and Semi-quantitative analysis based on XRD at 8 days and 8 months.

The application of this knowledge is suited for the characterization of NMt as a potential pozzolanic SCM can open a new horizon for the understanding of the effect and further development of nanoclays and NMt in cementitious composites and lime binders. Lastly, this study can further be elaborated for the development of new binders for cultural heritage conservation, referred to in detail in the discussion.

## **1. Materials and Methods**

### **1.1. Materials**

A commercially available lime putty was mixed at various concentrations with three aqueous dispersions of NMt as described below:

#### **1.1.1. Organomodified nano-montmorillonite dispersions (nC1 and nC2)**

A purified bentonite suspension [3.9% Mt and 96.1% water, Cation Exchange Capacity (CEC) 105 meq/100 g], produced by Laviosa Chimica Mineraria S.p.A., was organomodified by exchange of basal metal cations with methylbenzyl di-hydrogenated tallow ammonium chloride (Noramonium MB2HT) at Lietuvos Energetikos Institutas [18] producing NMt powder, named as XDB. This organomodified powder contained approximately 43% Noramonium MB2HT bound to the Mt and comprised the base for two organomodified dispersions. This proportion was confirmed by characterization of the starting material via thermogravimetric analyses as shown in the results section.

NMt powder XDB, was dispersed in water to avoid agglomeration, which would bring the material back to the micron scale. The side effect of the organomodification for cement chemistry is the creation of a hydrophobic nanocomposite, incompatible with water, causing extensive flocculation of particles, when dispersed. Surfactant technology was employed to leverage this fact and in specific:

- (1) 5% by mass (non-ionic) fatty alcohol and 1% by mass defoaming agent was used to create nC1 dispersion, and



(2) 5% by mass (anionic) alkyl aryl sulphonate was used to create nC2 dispersion.

The NMt loading achieved for both the aqueous dispersions was 15% XDB.

### **1.1.2. Inorganic nano-montmorillonite dispersion (nC3)**

The inorganic NMt powder used for the NMt dispersion is commercially available under the name Dellite®HPS. It was derived from the purification of bentonite by Laviosa Chimica Mineraria S.p.A. Dellite®HPS, is by nature compatible with water. However, the introduction of inorganic dispersant was necessary to overcome the electrostatic interaction of particles for high clay loading in aqueous solutions. Sodium polyphosphate was used for the dispersion of the inorganic NMt, in water. The NMt loading achieved in the aqueous dispersion was 15% HPS solids by total mass.

### **1.1.3. Lime Putty (LP)**

A commercially available lime putty (LP) conforming to class CL 90 according to BS EN 459-1 norm was used [19].

## **1.2. Methods**

### **1.2.1. Background**

It is acknowledged that a number of standardised pozzolanic reactivity tests are established such as the Chapelle method, Fratinni method and Strength Activity Index [20]. However, the

Chapelle method is primarily valid for calcined clays, because the consumption of calcium hydroxide is only related to the amorphous and vitreous phase of a material. To the best knowledge of the authors it has never been applied for the characterization of non-calcined NMt dispersions. Moreover, the Fratinni and Strength Activity Index method necessitate the use of cement, which is already a composite material. Therefore, for this work, an innovative method was introduced by which non-thermally treated NMt enhanced lime putty pastes were prepared, allowed to harden and examined via XRD, TGA/dTG and a semi-quantitative analysis based on XRD at an age of 8 days and 8 months. The pastes employed for the suggested method were preferred to the traditional ones for the following reasons; (i) lime putty constitutes a highly reactive binding materials in comparison to the dry powder CaO used for the Chapelle method. In addition to this, lime putty exhibits a higher specific surface area conferring not only greater reactivity but also better rheological properties particularly when aged [21,22] (ii) lime putty's composition is simple (chemically unbound water easily separated by drying at 100°C [23]) compared to the complex chemical composition of Portland cement clinker, which is necessary for the Fratinni method and the Strength Activity Index, (iii) binary compositions allow for straight forward conclusions and (iv) such studies broaden our current knowledge on materials' combination for historic lime mortar conservation. That said, the starting NMt powders (HPS and XDB) and two of the dispersions (nC2 and nC3) were tested with the Chapelle method for comparison and for validation of the newly introduced method.

## 1.2.2. Experimental Procedure

### The new method

A reference sample of LP was prepared by vigorous whisking of the material with a pallet knife until it was homogenized. 20 g of the plain LP sample were sealed in a vial.

100 g of the reference LP was dried at 60°C for 24 hours and another 100 g was dried at 100°C, to detect any differences in  $\text{Ca}(\text{OH})_2$  or surface water content. The procedure described in [23] was followed and the relationship established between lime slaking time and amount of free water was confirmed, i.e. after 24 hours of drying immediately after slaking the amount of free water measured reached 60% by mass in accordance with BS EN 459-1 [19] and suggestion by Moropoulou et al [24] that free water content should not exceed 60% by mass.

Six NMt modified lime putty pastes were prepared as shown in

Table 1. The mix proportions of NMt refer to the NMt dispersion rather than NMt solids only. Materials were manually mixed due to the small quantities required, with a spatula for 1 minute and the pastes were placed in vials. All vials were immediately sealed with their cap, protected with tape and further secured in a sealed, airtight bag to avoid contact with the  $\text{CO}_2$  present in air and consequently carbonation, in order to only study the pozzolanic reaction.

The only moment when the samples were in contact with air (i.e. when carbonation could have taken place by the formation of calcium carbonate), was during mixing of the pastes or during crushing or testing. Because these moments were quite limited and carbonation is a self-limiting reaction, it can be assumed that the amount of  $\text{CaCO}_3$  precipitated by carbonation is limited and can be disregarded for the 8-days-old pastes. If carbonation takes place then the hydrated

compounds (such as  $\text{Ca}(\text{OH})_2$  and calcium silicate hydrates (C–S–H) [25]) will also have been carbonated [26].

Samples were cured for two different periods: (i) 6 days at room temperature and consecutively oven-dried for 36 hours and tested at day 8 and (ii) 238 days at room temperature and consecutively oven-dried for 36 hours and tested at 8 months (240 days). Only the LP/nC3 pastes set immediately, whereas the remaining four formulations were still unhardened after the six-day period, as can be seen in Figure 1; the fact that nC3 exhibited a more pronounced binding activity could possibly be attributed to greater pozzolanicity (sample number 3 and 6 in Figure 1 and Table 1).

Table 1: Composition of LP/nC1, LP /nC2, LP/nC3 pastes

Sample	Sample No in Figure 1	LP content (% mass)	Dispersion content (% mass)
100% LP		100	0
50% LP + 50% nC1 dispersion	1	50	50
50% LP + 50% nC2 dispersion	2	50	50
50% LP + 50% nC3 dispersion	3	50	50
20% LP + 80% nC1 dispersion	4	20	80
20% LP + 80% nC2 dispersion	5	20	80
20% LP + 80% nC3 dispersion	6	20	80

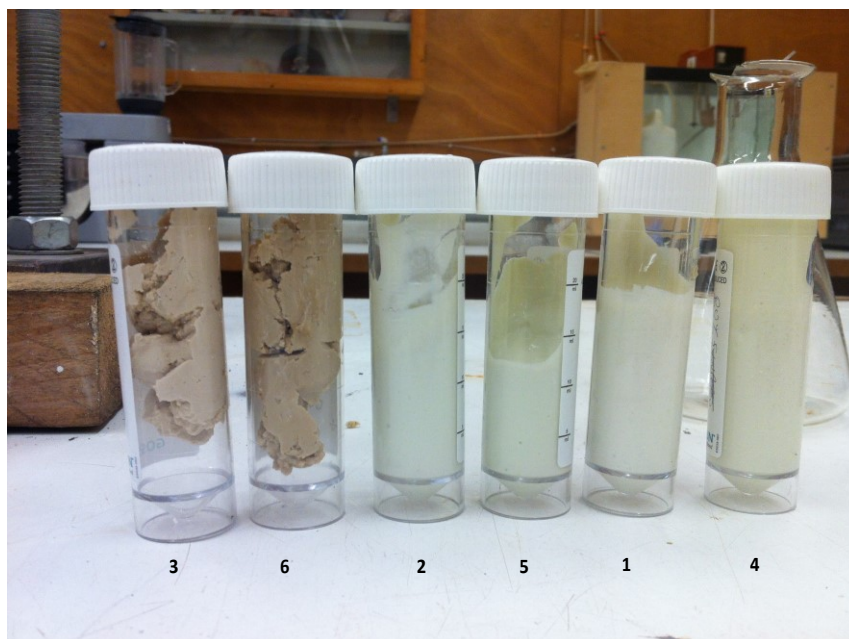


Figure 1: Characteristics of LP/nC1, LP /nC2, LP/nC3 pastes after six days of curing and before oven-drying

When the six-day period had passed, the pastes were oven-dried at 60°C for 24 hours. After oven drying was complete, the samples were crushed to powder passing through a 125  $\mu\text{m}$  sieve. It should be noted that the LP/nC2 as well as the LP/nC1 were extremely soft and fine upon grinding. On the contrary, the LP/nC3 pastes were very hard to break and to grind. Ground powdered samples were poured in vials and were allowed to dry for a further 12h in a desiccator (to avoid carbonation or sample contamination) placed in the oven at 60°C.

The procedure was repeated 8 months later for the study of the ageing process of the same pastes.

### Validation of the new method via the Chapelle test

The pozzolanic activity of the starting NMt powders [XDB (discussed in section 1.1.1) and Dellite®HPS (abbreviated as HPS and discussed in section 1.1.2)] and two of the dispersions (nC2 and nC3) were confirmed by the Chapelle test [27,28]; 1g of each sample was mixed with 1 g of Ca(OH)<sub>2</sub> and 100 ml of boiled water. The suspension was boiled for 16 h and the free Ca(OH)<sub>2</sub> was determined by means of sucrose extraction and titration with a HCl solution. Powders of the Chapelle products were tested via X-ray diffraction and compared with raw NMt powders and dispersions.

### **1.2.3 Analytical techniques**

Mineralogy was investigated via XRD and the thermal properties via TGA/dTG. The consumption of calcium hydroxide was further evaluated with the adoption of a semi-quantitative method.

### **X-ray diffraction (XRD)**

XRD measurements were performed using a D8 ADVANCE x-ray diffractometer with CuK<sub>α</sub> radiation. Spectra were obtained in the range  $4^{\circ} < 2\theta < 60^{\circ}$  at an angular step-size of  $0.016^{\circ} 2\theta$ . Analysis of reflections and d-value were calculated according to Bragg's law ( $n\lambda = 2d\sin\theta$ ) [29]. WiRE<sup>TM</sup> software [30] was used for mathematical curve fitting (polynomial smoothing) of the XRD diffractograms, and EVA software [31] was used to determine the mineralogy and

integrated area. The most matching compounds formed were selected based on the elemental analysis of the nano-montmorillonite dispersions [10].

#### **Thermal gravimetric analyses (TGA)**

Thermal gravimetric analyses (TGA) were carried out using a Setaram TGA92 instrument. 20 mg of each sample were placed in an alumina crucible and heated at a rate of 10°C/min from 20°C to 1000°C under 100 mL/min flow of inert nitrogen gas. The differential thermal gravimetric (TGA/dTG) curve was derived from the TG curve. Buoyancy effects were taken into account, by correcting the curves via automatic blank curve subtraction. TG analyses were carried out on oven-dried samples instead of wet ones. This was to differentiate, at 100-140°C, between the mass loss that may be attributed to the decomposition of calcium silicate hydrate, from the mass loss that may be attributed to water evaporation from the pores of the samples. Moreover, greater convergence with XRD results can be expected if samples are in the same state. Therefore, since XRD analysis must be carried out in powders, the same state was preferred for TGA.

#### **1.2.4. Mathematical elaboration**

##### Decomposition stages of LP/nC1, LP/nC2 and LP/nC3 pastes

In order for the method to yield results, the net amount of  $\text{Ca(OH)}_2$  consumed must be calculated. That is to say, the amount of NMt decomposing within the specific temperature range as that for  $\text{Ca(OH)}_2$  i.e. 400-500°C, must be subtracted from the total mass loss recorded by applying the following formulae:

$$M_{CH} = M_{loss}^{400-500} - M_{NMt}^{400-500} \times (\%NMt) \quad \text{Equation: 1}$$

Where,

$M_{CH}$  = Mass loss related to  $Ca(OH)_2$

$M_{loss}^{400-500}$  = Mass loss of LP/NMt paste recorded by TG between 400-500°C

$M_{NMt}^{400-500}$  = Mass loss of dried NMt recorded by TG between 400-500°C

(%NMt) = [% of NMt dispersion present in the paste (i.e. 50% or 80%)]

It is assumed that the mass loss of dried NMt recorded by TG between 400-500°C is proportional to its original percentage in the mix.

Accordingly, the net mass loss related to  $CaCO_3$  must be calculated by subtracting from the total mass loss the amount of NMt decomposing within the specific temperature range, i.e. 600-800°C, according to the following formulae:

$$M_{CC} = M_{loss}^{600-800} - M_{NMt}^{600-800} \times (\%NMt) \quad \text{Equation: 2}$$

Where,

$M_{CC}$  = Mass loss related to  $CaCO_3$

$M_{loss}^{600-800}$  = Mass loss of LP/NMt paste recorded by TG between 600-800°C

$M_{NMt}^{600-800}$  = Mass loss of dried NMt recorded by TG between 600-800°C

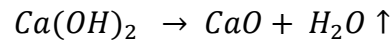
(%NMt) = [% of NMt dispersion present in the paste (i.e. 50% or 80%)]

As assumed above, the mass loss of dried NMt recorded by TG between 600-800°C is proportional to its original percentage in the mix.



304 Mass calculations

305 For the area associated with the dehydration of  $\text{Ca(OH)}_2$  between  $400^\circ\text{C}$  and  $510^\circ\text{C}$  the  
306 following chemical reaction applies:



307 The amount of  $\text{Ca(OH)}_2$  present in the paste at different ages can be computed by the  
308 stoichiometric elaboration of the mass loss results within the specific temperature range:

$$309 \quad MM_{CH} = \frac{M_{CH} \times 74.0930}{18.0153} \Rightarrow MM_{CH} = \frac{M_{CH}}{0.243} \quad \text{Equation: 3}$$

310 Where,

311  $MM_{CH}$  = mass of  $\text{Ca(OH)}_2$

312  $M_{CH}$  = Mass loss related to  $\text{Ca(OH)}_2$  measured by TGA

313  $18.0153 \text{ g/mol}$  = molecular mass of  $\text{H}_2\text{O}$  and  $74.0930 \text{ g/mol}$  = molecular mass of  $\text{Ca(OH)}_2$ .

314 Similarly, the decomposition of  $\text{CaCO}_3$  occurs between  $700^\circ\text{C}$  and  $810^\circ\text{C}$  according to the  
315 following chemical reaction [32]:



317 The amount of  $\text{CaCO}_3$  present in the paste at different ages can be computed by the  
318 stoichiometric elaboration of the mass loss results within the specific temperature range:

$$319 \quad MM_{CC} = \frac{M_{CC} \times 100.0869}{44.0100} \Rightarrow MM_{CC} = \frac{M_{CC}}{0.44} \quad \text{Equation: 4}$$

320 Where,

321  $MM_{CC}$  = mass of  $\text{CaCO}_3$

322  $M_{CC} = \text{Mass loss related to CaCO}_3 \text{ measured by TGA}$

323  $100.0869 \text{ g/mol} = \text{molecular mass of CaCO}_3 \text{ and } 44.0100 \text{ g/mol} = \text{molecular mass of CO}_2$

324

325 Carbonation recalculations

326 Furthermore, the reference LP paste and all LP/NMt pastes had carbonated. As a result, the total  
327 molar mass related to  $\text{Ca(OH)}_2$  had to be recalculated:

328

329 By assuming that all of this calcium carbonate (mass loss traced above  $600^\circ\text{C}$ ) was once  
330 calcium hydroxide:

331  $\text{Ca(OH)}_2 + \text{CO}_2 \rightarrow \text{CaCO}_3 + \text{H}_2\text{O}$

332 Which in molar mass terms is:  $74.0930 + 44.0100 \rightarrow 100.0869 + 18.0153$ , therefore:

333 Mass of  $\text{Ca(OH)}_2$  that has carbonated =  $MM_{\text{carbCH}} = [MM_{CC}] / [(100.0869 / 74.0930)] = MM_{CC} /$

334 1.35

335 Therefore:

336  $MM_{\text{totCH}} = MM_{\text{CH}} + MM_{\text{carbCH}}$  Equation: 5

337 Where,

338  $MM_{\text{totCH}} = \text{Total mass of Ca(OH)}_2 \text{ prior to carbonation}$

339  $MM_{\text{CH}} = \text{Mass of Ca(OH)}_2 \text{ as calculated by Equation 3}$

340  $MM_{\text{carbCH}} = MM_{\text{CC}} / 1.35 = \text{Mass of Ca(OH)}_2 \text{ that has carbonated (i.e. mass loss traced above}$   
341  $600^\circ\text{C as calculated by Equation 2 and 4)}$

## 342 **2. Results and Discussion**

### 343 **2.1. X-ray Diffraction (XRD)**

344 The consumption of  $\text{Ca(OH)}_2$  (Portlandite or CH) by the three different NMt dispersions was at  
345 first confirmed by XRD analyses carried out at both 8-day and 8-month old powders (Figure 2).  
346 In terms of mineral and phase identification, Montmorillonite particles with  
347 different sizes, have been differentiated according to previous work carried out by the authors  
348 [10]. Graphs A and B identify a peak as being Mt. Diffractograms show that reflections assigned  
349 to Portlandite reduce with time. Moreover, the higher the nC1, nC2 or nC3 content the greater  
350 the Portlandite consumption. This reduction was more pronounced for nC3. In fact, in  
351 agreement with the TG analysis which follows, Portlandite almost disappeared for the  
352 20%LP80%nC3 paste at day 8, whereas for month 8 it was completely eliminated. Interestingly,  
353 nC3 showed high crystallization with montmorillonite and Portlandite reflections transforming  
354 into sodalite, calcium silicate and carbsite for the 50%LP50%nC3 paste at 8 months and  
355 significant quantities of calcium aluminum oxide carbonate hydrate, a major cementing  
356 compound [33] for the 20%LP80%nC3 paste at month 8.

357 Dispersions nC1 and nC2 exhibited similar  $\text{Ca(OH)}_2$  consumption, with nC1 being slightly  
358 more reactive towards the production of calcium-containing hydrate compounds. In fact, the C–  
359 S–H is amorphous and its presence may be recorded by humps appearing between  $20$  and  $30^\circ 2\theta$   
360 [2,34]. All XRD spectra of the LP/NMt pastes present such a hump approximately at  $20^\circ 2\theta$ , that

is to say, after the Portlandite peak at  $18.2^{\circ}2\theta$ . In fact, for all nC2 enhanced pastes only the C–S–H humps were identified and no crystal compounds were detected.

Furthermore, of strätlingite  $[\text{Ca}_2\text{Al}((\text{AlSi})_{1.11}\text{O}_2)(\text{OH})_{12}(\text{H}_2\text{O})_{2.25}]$  were traced for the 50%LP50%nC1 paste at 8 days and quantities of C–S–H were identified for the 20%LP80%nC1 paste at day 8. At this point it should be noted there has been a debate on the nature of the C–S–H structure and it has recently been postulated, that although amorphous, at the nanolevel it exhibits a highly ordered structure [25]. Therefore, it is possible that even by XRD analyses, diffractions recorded as humps can assist towards the validations of such findings. After 8 months, it seems that montmorillonite was transformed into Stichtite  $[\text{Mg}_6\text{Cr}_2\text{CO}_3(\text{OH})_{16} \cdot 4\text{H}_2\text{O}]$  for both 50%LP50%nC1 and 20%LP80%nC1 pastes.

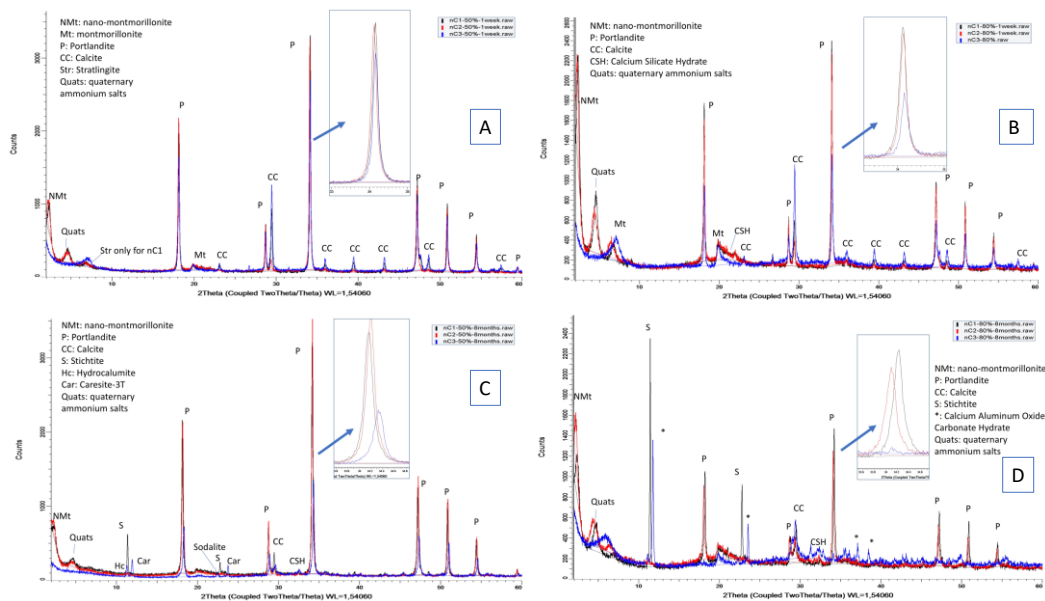


Figure 2: XRD analyses of (A) 50%LP+50%nC1/nC2/nC3 dispersions - at day 8, (B): 20%LP+80%nC1/nC2/nC3 dispersions - at day 8, (C) 50%LP+50%nC1/nC2/nC3 dispersions - at month 8 and (D) 20%LP+80%nC1/nC2/nC3 dispersions - at month 8

## 2.2. Semi-quantitative analysis based on XRD

A semi-quantitative analysis was developed on the grounds of comparison of the integrated areas (wide rectangle in Figure 3) under the two adjacent reflections of  $\text{Ca(OH)}_2$  at  $28.7^\circ 2\theta$  and  $\text{CaCO}_3$  at  $29.4^\circ 2\theta$ . Polynomial curve fitting was performed to smoothen the XRD results and even out minor noise (as seen in Figure 3). The calcite traced in the nC3 enhanced pastes just below  $30^\circ 2\theta$  angle, is attributed to the Mg-calcite naturally present in Mt, whereas the calcite identified in nC1 enhanced pastes can be related to the high quantities of organic matter traced in the characterization of the starting nano-montmorillonite powders [9]. For the 8-month-old pastes the presence of  $\text{CO}_3$  containing compounds is typical of carbonation process [33]. The reduction of the Portlandite peak can only be compared between the same LP content pastes and no comparisons should be made between the 50% and 80% nC content pastes because the starting Portlandite (CH) is different. Therefore, for day 8, none of the 50%LP pastes showed significant reduction, whereas for the 20%LP pastes, nC3 dispersion showed the highest consumption (lowest relative peak intensity in Figure 3). Similarly, for month 8, nC3, followed by nC1, showed the highest CH consumption for the 50%LP pastes, whereas for the 20%LP pastes, CH was extinct in the nC3 enhanced pastes.

Next, EVA software [31] was used for the determination of the areas under the  $28.7^\circ 2\theta$  and  $29.4^\circ 2\theta$  angles' peak. The integrated area comprises the total area under both adjacent reflections. The results of these analyses are depicted in Figure 4, with the consumption of  $\text{Ca(OH)}_2$  clearly identified particularly by nC3 enhanced pastes in both ages. It can be, hence, concluded that XRD can give an estimation on the quantities of CH and calcium carbonate present in the bulk powder sample, however a more elaborate procedure is still required in order to differentiate the performance particularly of the organomodified dispersions, nC1 and nC2.

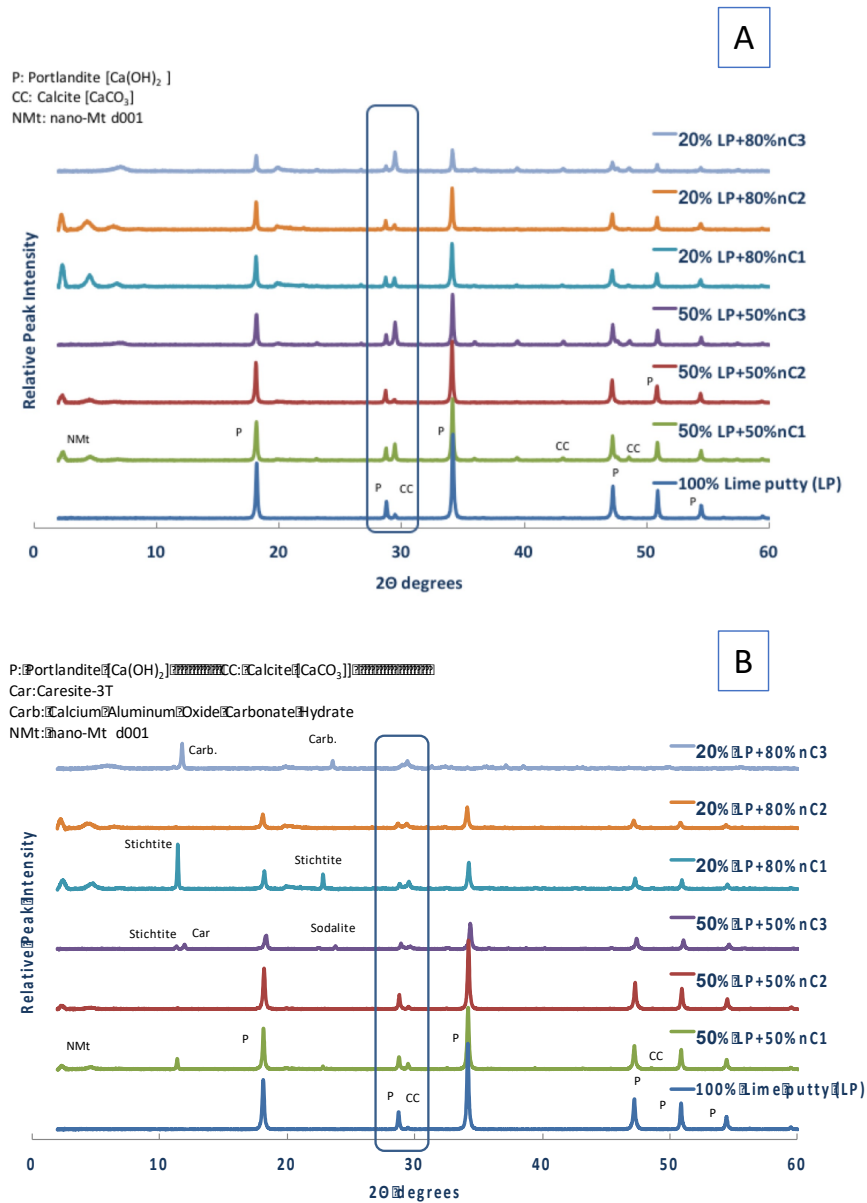


Figure 3: Investigation of pozzolanic activity: XRD analyses of LP/nC1, LP/nC2 and LP/nC3 pastes (A) at day 8 and (B) at month 8

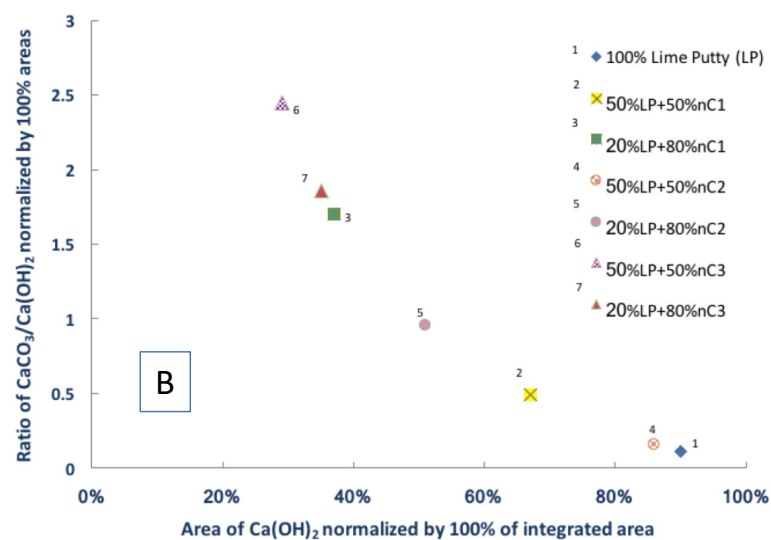
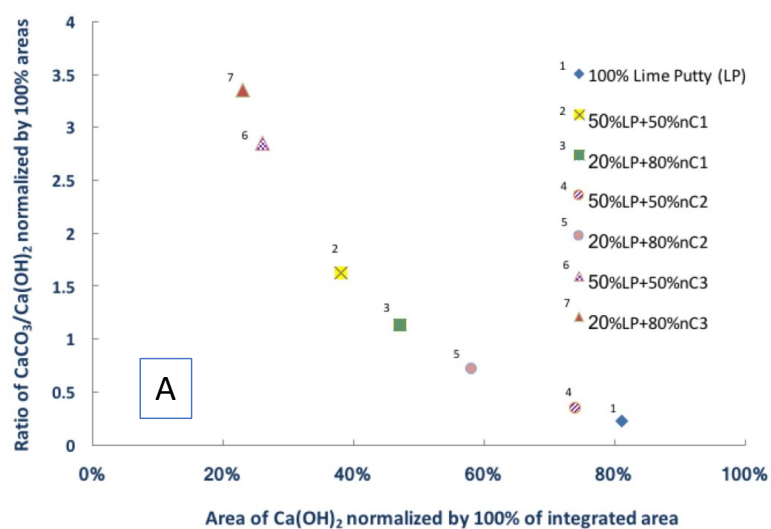


Figure 4: Results of semi-quantitative XRD analyses of LP/nC1, LP/nC2 and LP/nC3 pastes (A) at day 8 and (B) at month 8

## 2.3. Thermal gravimetry

First of all, the decomposition stages of lime putty were studied. Next, for the decomposition of the raw NMt dispersions data was derived from published research [9,10] and lastly, the decomposition of the NMt enhanced lime putty pastes was scrutinized and discussed.

### (i) Decomposition of lime putty paste

All results shown correspond to pastes pre-dried at 60°C. Additionally, only the reference (pure LP) paste, was pre-dried at 60°C and at 100°C and thermogravimetrically analysed for comparison (Figure 5), as suggested by [23]. It was found that pre-drying LP at 100°C almost drained it from surface water, therefore the TGA showed marginal mass loss up to 100°C. However, slightly greater amount of surface water was lost up to 100°C on TGA for the lime putty pre-dried at 60°C, as expected. Most importantly, pre-drying at either temperature did not affect the detection of pure  $\text{Ca(OH)}_2$  content which was found to reach almost 90% by mass. In agreement with the study of [23] in which, one-month old lime putty lost free and adsorbed water (3.5%) up to 300°C, the chemically bound water (21.5%) related to  $\text{Ca(OH)}_2$  content up to 550°C and mass (2.3%) related to decomposition of  $\text{CaCO}_3$  above 600°C, in this study the mass losses were recorded at similar temperature ranges and exhibited almost equal mass losses related to  $\text{Ca(OH)}_2$  and  $\text{CaCO}_3$  content, implying that the lime putty had slightly carbonated (Table 2).



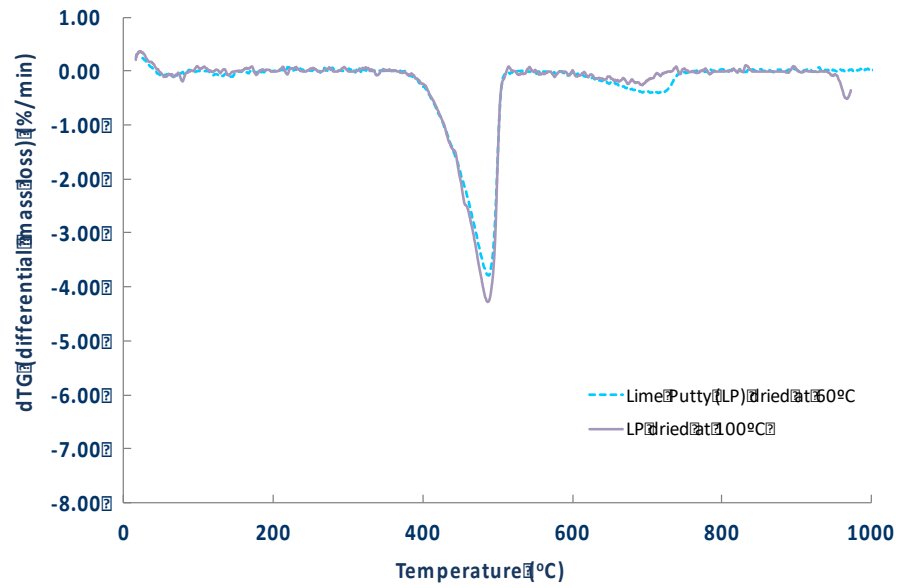


Figure 5: Comparison of dTG curves of LP dried at different temperatures

Table 2: dTG recorded mass loss (%) of lime putty

Sample	100-	200-	300-	400-	600-	800-
	200°C	300°C	400°C	600°C	800°C	1000°C
Dried 100% LP at day 8	0.33		20.20		3.52	0
Dried 100% LP at month 8	0.33		21.24		1.62	0

**At day 8:**

(1)  $\Rightarrow M_{CH}^{LP} = 20.2\%$ , therefore following equation 3:  $MM_{CH}^{LP} = 20.2/0.243 = 83.13$

432 (2)  $\Rightarrow M_{CC}^{LP} = 3.52\%$ , therefore following equation 4:  $MM_{CC}^{LP} = 3.52/0.44 = 8.0$

433  $MM_{carbCH}^{LP} = MM_{CC} / 1.35 = 8/1.35 = 5.93$

434 Following equation 5:  $MM_{totCH}^{LP} = 83.13 + 5.93 = 89.06$

435 Therefore, **for 50%LP:  $MM_{totCH}^{LP} = 44.53$  and for 20%LP:  $MM_{totCH}^{LP} = 17.82$**

436 **Accordingly, at month 8:**

437 (1)  $\Rightarrow M_{CH}^{LP} = 21.2\%$ , therefore following equation 3:  $MM_{CH}^{LP} = 21.2/0.243 = 87.24$

438 (2)  $\Rightarrow M_{CC}^{LP} = 1.6\%$ , therefore following equation 4:  $MM_{CC}^{LP} = 1.6/0.44 = 3.7$

439  $MM_{carbCH}^{LP} = MM_{CC} / 1.35 = 3.7/1.35 = 2.74$

440 Following equation 5:  $MM_{totCH}^{LP} = 87.24 + 2.74 = 89.98$

441 Therefore, **for 50%LP:  $MM_{totCH}^{LP} = 45.0$  and for 20%LP:  $MM_{totCH}^{LP} = 18.0$**

442

443 (ii) Decomposition of raw nC1, nC2, nC3 dispersions

444 The qualitative interpretation of the decomposition stages of the three raw NMt dispersions is  
445 described in an earlier paper [10].

446 With respect to the organomodified NMt dispersions it is known that the modifier of the starting  
447 NMt powder (XDB) was intended to be fully decomposed by 500°C (resulting in a loss of 43%  
448 by mass, as mentioned in section 2.1.1 and 2.1.2). Three peaks are identified via differential  
449 thermal gravimetry analyses of nC1 and nC2 dispersions: (i) at 70°C, related to the loss of free  
450 water (ii) at 200°C assigned to the decomposition of the modifier and (iii) at 360°C assigned to  
451 loss of the modifier molecules physically adsorbed on the surface of the Mt layers with a

shoulder at around 410°C for nC1 or the main peak without any shoulders at 410°C for nC2, attributed to deconstruction of the modifier bound to the interlayer of the NMt [10]. In terms of quantitative analysis of the mass losses recorded during the various temperature intervals, differential thermal gravimetry analysis of nC1 and nC2 dispersion yielded the following results [35]:

Table 3: dTG analysis recorded mass loss (%) of nC1 and nC2 dispersions

Sample	0- 100°C	100- 180°C	180- 280°C	280- 400°C	400- 500°C	500- 600°C	>600°C
Dried 100% nC1	0.68	2.63	6.73	<u>35.34</u>	<u>9.48</u>	2.17	0.00
Dried 100% nC2	1.02	1.82	6.52	<u>25.95</u>	<u>20.14</u>	2.29	0.00

It should be noted that for nC1 the mass loss between 280-500°C was equal to 44.8%, whilst for nC2 the mass loss between 280-500°C was equal to 46.1%. These were both slightly higher than the theoretical loss of mass of 43%. Moreover, there are traces of mass lost between 500-600°C. These mass losses can be attributed to the decomposition of the surfactants. For nC1 the surfactant and antifoam used is known to decompose below 400°C, whereas the surfactant used for nC2, the alkyl aryl sulphonate, is known to decompose at 580°C.

The inorganic dispersion nC3 exhibited different behaviour, therefore the thermal decomposition involved less stages than the organomodified dispersions (Table 5). Three peaks were present; one at 85°C with a shoulder at 110°C due to the loss of adsorbed water, a broader peak at 650°C and a sharp peak at 750°C which may be attributed to the loss of structural water

– dihydroxylation of the Mt. The complete deconstruction of the Mt (loss of 4% by mass) took place between 600-800°C as also reported in literature [6,36,37]. It should be noted, though, that the dispersant used for nC3, the tripolyphosphate, also decomposes at 600°C [10].

Differential thermal gravimetry analysis of nC3 dispersion yielded the following mass losses [35]:

Table 4: dTG analysis recorded mass loss (%) of nC3 dispersion

Sample	0- 100°C	100- 180°C	180- 300°C	300- 600°C	600- 800°C	800- 1000°C
Dried 100% nC3	10.82	5.34	1.00	1.00	3.30	1.13

(iii) Decomposition of LP/nC1, LP/nC2 and LP/nC3 pastes

The pastes were thermogravimetrically analysed at 8 days and at 8 months (Figure 6). XRD analyses is required for the determination of the various compounds which decompose at similar temperature intervals.

For the temperature range between 20-100°C all free water was evaporated. For the temperature range between 110-400°C: The pozzolanic reaction between lime putty and NMt dispersions produced hydrates similar to the ones found in literature for lime/metakaolin pastes; calcium silicate hydrates (C–S–H), decomposing between 110-140°C, strätlingite (C<sub>2</sub>ASH<sub>8</sub>) decomposing between 140-200°C and C<sub>4</sub>ASH<sub>13</sub> decomposing between 200-270°C and C<sub>3</sub>ASH<sub>6</sub>

decomposing between 270-380°C [38,39]. Indeed, strätlingite and other calcium-containing hydrates were also confirmed in this research via XRD analysis.

Moreover hydrocalumite a carbonate compound traced via XRD in the 50%LP50%nC3-8 month-old paste, undergoes dihydroxylation between 200-400°C [40].

Furthermore, stichtite traced via XRD in the 50%LP50%nC1 and 20%LP80%nC1 -8 month-old paste, and caresite-3T (another carbonate) traced via XRD in the 50%LP50%nC3-8 month-old paste, also decomposed within this temperature range [41], although for stichtite other researchers state 550 and 670°C as the main peaks signalling its decomposition [42].

Lastly, calcium aluminium oxide hydrate carbonate mainly decomposed between 180-280°C, which justified the increased mass loss within this temperature range for the nC3 enhanced pastes [33].

For the temperature range between 400-500°C the consumption of  $\text{Ca(OH)}_2$  could not be clearly observed in the early age thermograms at day 8, analytical elaboration was necessary. At month 8 all the higher nC content pastes showed pozzolanic reactivity. However, only the 20%LP+80%nC3 at month 8 clearly showed extinction of  $\text{Ca(OH)}_2$  towards significant production of hydrates (Figure 6 (D) to (F)). For the remaining pastes, including all early age ones, judging whether  $\text{Ca(OH)}_2$  was consumed or not was not obvious from the thermographs because between 400-500°C two parts were decomposing towards the production of hydrates:

- nC1/nC2 dispersions (containing the modifier and Mt), which fully decomposed by 500°C
- and  $\text{Ca(OH)}_2$

512 Moreover, although minor carbonation has taken place for the 8-month old samples as  
513 witnessed by the endothermic peak present at approximately 730°C, the calculation of the  
514 amount of CaCO<sub>3</sub> produced was intricate because above 600°C three parts were decomposing:

- 515 • nC3 containing the surfactant (tripolyphosphate) and Mt
- 516 • calcite typically traced in montmorillonites [9]
- 517 • and CaCO<sub>3</sub> due to the carbonation of Ca(OH)<sub>2</sub>

518  
519 For the temperature range above 800°C, no formation of high temperature silicate minerals e.g.  
520 cristobalite, mullite or spinel was detected either at day 8 nor at month 8 via XRD analyses.  
521 Other CO<sub>3</sub>-containing compounds of the 8-month-old pastes were detected via XRD, such as  
522 sodalite, which decomposes above 840°C [43] and calcium aluminium oxide hydrate carbonate  
523 which decomposes above 800°C [33].

524  
525 As a concluding remark the temperature range 400-500°C selected for assessing if Ca(OH)<sub>2</sub> was  
526 consumed or not encompassed the decomposition of Ca(OH)<sub>2</sub> and nC1/nC2 and the temperature  
527 range 600-800°C selected for recalculations for carbonation, encompassed the decomposition of  
528 CaCO<sub>3</sub> (Mg-calcite and calcite) and nC3.

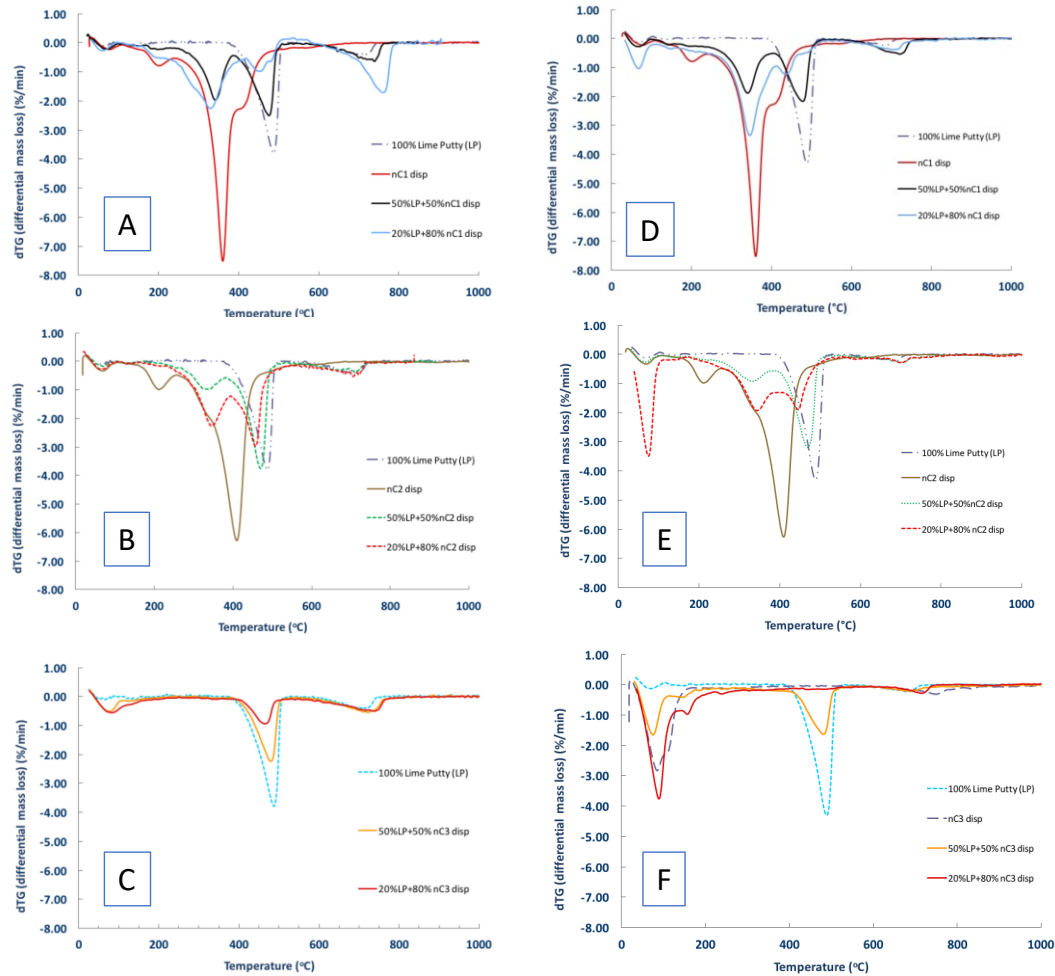


Figure 6: TGA for (A) LP/nC1, (B) LP/nC2, (C) LP/nC3 pastes at 8 days and (D) LP/nC1, (E) LP/nC2, (F) LP/nC3 pastes at 8 months

Table 5 and Table 7 contain the exact mass loss of the LP/nC pastes recorded at the various temperature intervals, by the TG analyser. For the net amount of  $\text{Ca(OH)}_2$  consumed up to  $500^\circ\text{C}$ , the amount of nC1, nC2 or nC3 present must be deducted from the mass loss recorded by the TG analyser (Table 5 and Table 7) for the decomposition of the NMt enhanced lime putty pastes within the specific temperature range.

Respectively, for the net amount of  $\text{CaCO}_3$  detected due to carbonation of a part of  $\text{Ca(OH)}_2$  the amount of nC3 decomposing between  $600\text{--}800^\circ\text{C}$  must be deducted from the mass loss recorded by the TG analyser (Table 5 and Table 7) within the specific temperature range.

Table 5: dTG recorded mass loss (%) of LP/nC1, LP/nC2 and LP/nC3 pastes - at day 8

Sample	0- 100°C	100- 200°C	200- 300°C	300- 400°C	400- 500°C	500- 800°C	800- 1000°C
Dried 50% LP + 50% nC1	0.64	1.06	2.8	<u>10.53</u>	<u>13.97</u>	5.93	0
Dried 50% LP + 50% nC2	0.36	0.20	2.04	<u>7.35</u>	<u>18.63</u>	4.19	0
Dried 50% LP + 50% nC3	2.34	0.60	0.56		8.88	11.73	0
Dried 20% LP + 80% nC1	0.21	1.68	8.72	14.29	12.72	12.34	0
Dried 20% LP + 80% nC2	0.74	0.46	3.30	15.54	16.11	6.46	0
Dried 20% LP + 80% nC3	4.13	2.34	0.83		3.60	9.00	0

Estimating the theoretical mass loss related to the CH required analytical calculations, presented in the appendix for the ease of the reader. The results of these calculations are compared to the recorded values by the TGA Table 6. Theoretical and experimental values corroborated well at 8 days. The first column of Table 6 presents the results of  $M_{CH}$  of the Appendix table 2. The second column of Table 6 contains the recordings for temperature range 400-500°C presented in Table 5.

Table 6: Theoretical and experimental mass loss (%) of LP/nC1, LP/nC2 and LP/nC3 pastes related to CH consumption - at day 8

Sample	Theoretically expected mass loss (%)	Experimentally attained (TGA) mass loss (%)	Mass loss reduction related to CH consumption
50%LP+50%nC1	14.8	13.97	5.6%
50%LP+50%nC2	20.2	18.63	7.8%
50%LP+50%nC3	10.6	8.88	16%
20%LP+80%nC1	11.6	12.72	-
20%LP+80%nC2	20	16.11	20%
20%LP+80%nC3	4.8	3.60	25%



Similarly, the experimental mass losses recorded at the different temperature intervals for the 8-month-old pastes are presented in Table 7 and the theoretical mass loss related to the CH (analytically calculated in the appendix) are presented in

Table 8. Theoretical and experimental values corroborated well for the 50%LP and 50% nC1 or nC2 or nC3 dispersions. at 8 months. For the higher NMt content combinations, the experimentally attained mass loss (by the TGA/dTG) was significantly greater than the theoretically expected. This could indicate a significant pozzolanic activity with increased NMt quantities, given the time. In fact, at approximately 275°C and above 455°C dehydroxylation of stichtite and caresite which were previously detected via XRD at the 8 months old samples, occurs [44]. Hydrocalumite also decomposes within 400-500°C [40]. Lastly, calcium aluminate carbonate hydrates decompose mostly at 220 °C and 260 °C [33].

Table 7: dTG recorded mass loss (%) of LP/nC1, LP/nC2 and LP/nC3 pastes at month 8

Sample	0- 100°C	100- 200°C	200- 300°C	300- 400°C	400- 500°C	500- 800°C	800- 1000°C
Dried 50% LP + 50% nC1	0.83	1.55	3.71	<u>10.93</u>	<u>12.47</u>	5.57	0
Dried 50% LP + 50% nC2	0.81	0.76	2.86	<u>6.90</u>	<u>17.26</u>	3.40	0
Dried 50% LP + 50% nC3	5.43	2.38	2.66		9.23	2.94	0.34
Dried 20% LP + 80% nC1	3.46	2.70	5.81	20.68	8.10	5.50	0
Dried 20% LP + 80% nC2	10.18	1.45	4.34	14.46	11.37	4.93	0
Dried 20% LP + 80% nC3	13.45	6.65	3.96		1.42	3.00	0

Table 8: Theoretical and experimental mass loss (%) of LP/nC1, LP/nC2 and LP/nC3 pastes related to CH consumption - at month 8

Sample	Theoretically expected mass loss (%)	Experimentally attained (TGA) mass loss (%)	Mass loss reduction related to CH consumption
50%LP+50%nC1	15.4	12.5	19%
50%LP+50%nC2	20.7	17.3	16.8%
50%LP+50%nC3	11.1	9.3	16.8%
20%LP+80%nC1	11.8	8.1	31.4%
20%LP+80%nC2	20.4	11.4	44.3%
20%LP+80%nC3	5	1.4	71.6%

Deducting the mass loss related to the Mt decomposition from the mass loss recorded by the TG analyser required analytical calculations, presented in the appendix for the ease of the reader. The results of these calculations in terms of mass loss and molar mass are introduced in Table 9 and

Respectively, the experimental  $MM_{totCH}$  is given in the appendix, Table Ap-3. The theoretical  $MM_{totCH}$  is given in the appendix, Table Ap-4.

Table 10. The experimental  $MM_{totCH}$  is given in the appendix, Table Ap-1. The theoretical  $MM_{totCH}$  is given in the appendix, Table Ap-2.

Table 9: Results of mass loss and total molar mass of CH ( $MM_{totCH}$ ) [equation 1-5] at day 8

Sample	Experimental $MM_{totCH}$ Eq5	CRITERION	Theoretical $MM_{totCH}$	Pozzolanic behaviour [Yes (Y)/No (Y)/ equal (=)]
50%LP+50%nC1	47.85	<	60.91	Y
50%LP+50%nC2	42.44	<	83.13	Y

<b>50%LP+50%nC3</b>	50.56	=	50.32	=
<b>20%LP+80%nC1</b>	40.17	<	47.74	Y
<b>20%LP+80%nC2</b>	10.94	<	82.30	Y
<b>20%LP+80%nC3</b>	20.78	<	26.75	Y

583

584 Respectively, the experimental  $MM_{totCH}$  is given in the appendix, Table Ap-3. The theoretical  
585  $MM_{totCH}$  is given in the appendix, Table Ap-4.

586 Table 10: Results of mass loss and total molar mass of CH ( $MM_{totCH}$ ) [equation 1-5] at month 8

<b>Sample</b>	Experimental $MM_{totCH}$ <b>Eq5</b>	CRITERION	Theoretical $MM_{totCH}$	Pozzolanic behaviour [Yes (Y)/No (Y)/equal (=)]
<b>50%LP+50%nC1</b>	41.18	<	63.37	Y
<b>50%LP+50%nC2</b>	35.31	<	85.19	Y
<b>50%LP+50%nC3</b>	37.16	<	52.41	Y
<b>20%LP+80%nC1</b>	11.39	<	48.56	Y
<b>20%LP+80%nC2</b>	8.29	<	83.95	Y
<b>20%LP+80%nC3</b>	2.55	<	27.65	Y

587

588 From the elaboration presented above, the complexity of assessing the pozzolanic potentials of  
589 LP/nC1 or LP/nC2 or LP/nC3 pastes is demonstrated and resolved. It can be interpreted from  
590 the TG analyses that the higher NMt concentrations at 8 months can lead to the elimination of  
591  $Ca(OH)_2$  and that in all cases nC3 showed the highest pozzolanic activity, followed by nC2.  
592 With respect to the comparison between the performance of nC1 and nC2, it can be claimed that  
593 the better dispersed NMt particles, nC2, as tested by TGA, XRD and transmission electron  
594 microscopy imaging and crystallographic analyses [10] seem to be developing more stable  
595 bonds when participating in hydration reactions. The bulk of the material decomposes at higher  
596 temperature ranges (over 400°C) than nC1, which starts to decompose at 300°C. Possibly, the  
597 carbon molecules inserted within the platelets of nC2 that were intended to keep them apart did

not function as such, avoiding re-agglomeration of the NMt platelets. Furthermore, they possibly prevented carbonates from forming, as the LP/nC2 pastes did not show signs of carbonation at either age. On the contrary, the NMt particles of nC1, which by the abovementioned materials characterization techniques were found to be re-agglomerating and covered in an excess of organic matter [10], exhibited less stable bonds, decomposing at a lower temperature band and engaged in carbonation reactions with various carbonaceous compounds being formed.

#### **2.4. XRD analyses of raw NMt and Chapelle products**

The pozzolanic activity of the samples was confirmed by XRD analyses of the raw powders [9] XDB (Figure 7A) and HPS (Figure 7E) compared with their Chapelle products Chap-XDB (Figure 7B) and Chap-HPS (Figure 7F). Most importantly the XRD analyses of the raw NMt dispersions [10] nC2 (Figure 7C) and nC3 (Figure 7G) compared with their Chapelle products Chap-nC2 (Figure 7D) and Chap-nC3 (Figure 7H), are also presented. To the best knowledge of the authors this is the first time that the Chapelle method was used for testing the pozzolanic activity of non-calcined nano-montmorillonite dispersions. The following phases were identified in the raw dispersions: montmorillonites and feldspars for nC2 (Figure 7C) and sodium calcium magnesium aluminum silicate hydrate, sodium aluminum silicate hydroxide, calcite and feldspars for nC3 (Figure 7G). The reaction of 1 g of nC dispersion with 1 g of  $\text{Ca}(\text{OH})_2$  and 100 ml of boiled water yielded sodium calcium magnesium aluminum silicate hydrate and calcite for Chap-nC2 (Figure 7D) and calcium aluminum silicate hydroxide (CASH)/katoite and saponite for Chap-nC3 (Figure 7H). Both CASH and katoite (a low silica hydrogarnet) have been identified as products of pozzolanic reactions under hydrothermal conditions [45,46]. Furthermore, according to Gameiro et al who also traced katoite in their lime-metakaolin mortars, they concluded that this phase decreases together with calcium hydroxide as the age of

622 the mortar advances [47]. More importantly, it has been postulated that katoite is more resistant  
623 to carbonation than other salts formed during pozzolanic reactions [48]. Lastly, it is worth  
624 noting that the nano-montmorillonite dispersions bear significant resemblance to the starting  
625 powders they emerged from. Therefore, the nano-montmorillonite and montmorillonite,  
626 feldspar, calcite and quartz detected in XDB (Figure 7A) produced a significant amount of  
627 calcite and sodium calcium magnesium aluminum silicate hydrate under the Chapelle test  
628 (Figure 7B). In fact, this result is in absolute accordance with studies on nC2 modified  
629 composite cement formulations, in which significant amounts of calcite were traced via XRD  
630 and thermal-gravimetric analyses [8]. This is one of the main reasons for which the  
631 organomodified nano-montmorillonite dispersions have been found less favourable when added  
632 to cement pastes. On the contrary, the inorganic montmorillonite HPS which contained  
633 montmorillonite, calcite, quartz, feldspar and magnesium aluminium silicates (Figure 7E) also  
634 reacted with  $\text{Ca(OH)}_2$  in boiled water, producing ample CASH and katoite, clearly showing that  
635 the inorganic montmorillonite, be it raw or dispersed, has pozzolanic properties.

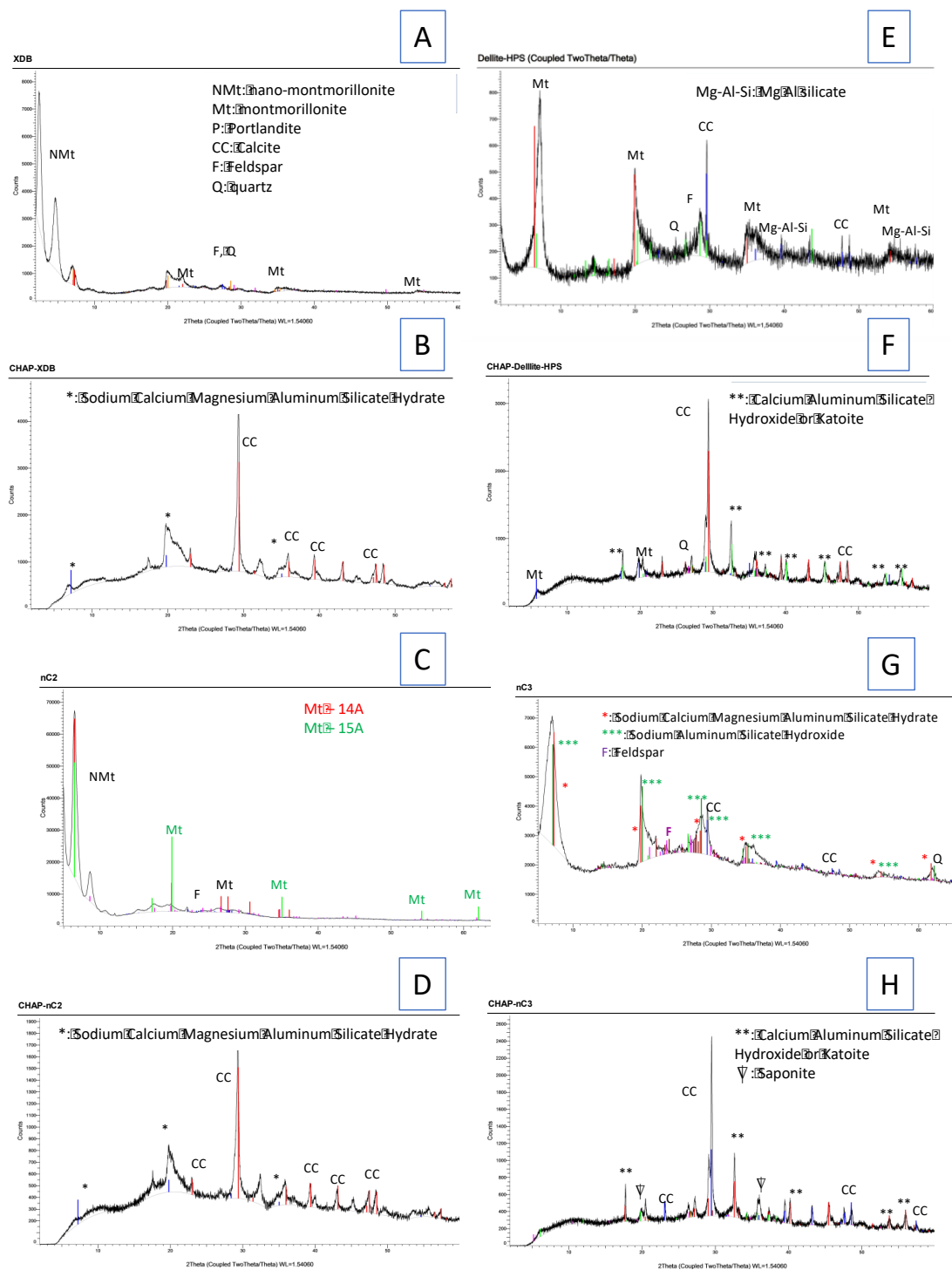


Figure 7: XRD for (A) XDB, (B) Chapelle-XDB, (C) nC2 , (D) Chapelle-nC2, (E) HPS, (F) Chapelle-HPS, (G) nC3, (H) Chapelle-nC3

### 3. Discussion

Lime putty, rich in  $\text{Ca(OH)}_2$  is a traditional building material used for centuries and still preferred to date for historic building conservation [24] particularly against Portland cement which is found in many cases highly incompatible with historic lime mortar masonry monuments [22]. However, current codes require that existing masonry structures must be retrofitted in order to withstand a combination of loads, for which increased mortar strength may offer a partial retrofitting upgrade. Given that Portland cement is avoided in historic mortar conservation, nano-montmorillonite could be used as an alternative binding pozzolanic and nanostructural reinforcing agent. Furthermore, NMt dispersions comprise even more interesting nanoreinforcement as they are easier to handle and can be more homogeneously dispersed in binders. In addition, the irreversible colloidal behaviour of lime putty has been linked to the oriented aggregation occurring during drying of the lime putty. While transmission electron microscopy imaging and crystallography support this finding, field emission scanning electron microscopy has also revealed plate-like nanoparticles of  $\text{Ca(OH)}_2$  clustering up to micron-sized elements. Slaked lime putty is, therefore, postulated to be compatible in terms of micro and nanostructure with NMt particles, which when dispersed comprise of nano-thick platelets individually available for reactions [4,10].

Recently published research conducted by the authors, on the nanostructure of the NMt dispersions [10] and characterization via TEM imaging and crystallography, XRD, SEM/EDX and TGA/DTG also taking into consideration results published in cement pastes [8] revealed that in nC1 the platelets were not fully exfoliated, and were possibly re-agglomerating in cement paste. This re-agglomeration increased the size of the particles to the micro-level, creating voids and allowing cracks to easily propagate in the hydrating cement pastes. It was concluded that

the surfactant used in this dispersion rendered the resulting pastes less resistant in both tension and compression.

With respect to nC2, platelets were found to be partially exfoliated, with several platelets intercalated in the volume of the dispersion. Overall, NMt platelets were better dispersed in water with the use of the anionic surfactant [10], which also significantly affected the mechanical performance of the nC2 enhanced Portland-limestone pastes [8]. It was concluded that the higher energy bonds between the NMt platelets and the anionic surfactant kept the platelets apart, while not allowing their slippage and crack evolution. A tortuous crack pattern, was developed, leading to more ductile behaviour and flexural strength improvements, still presenting areas of weakness due to some agglomeration of particles.

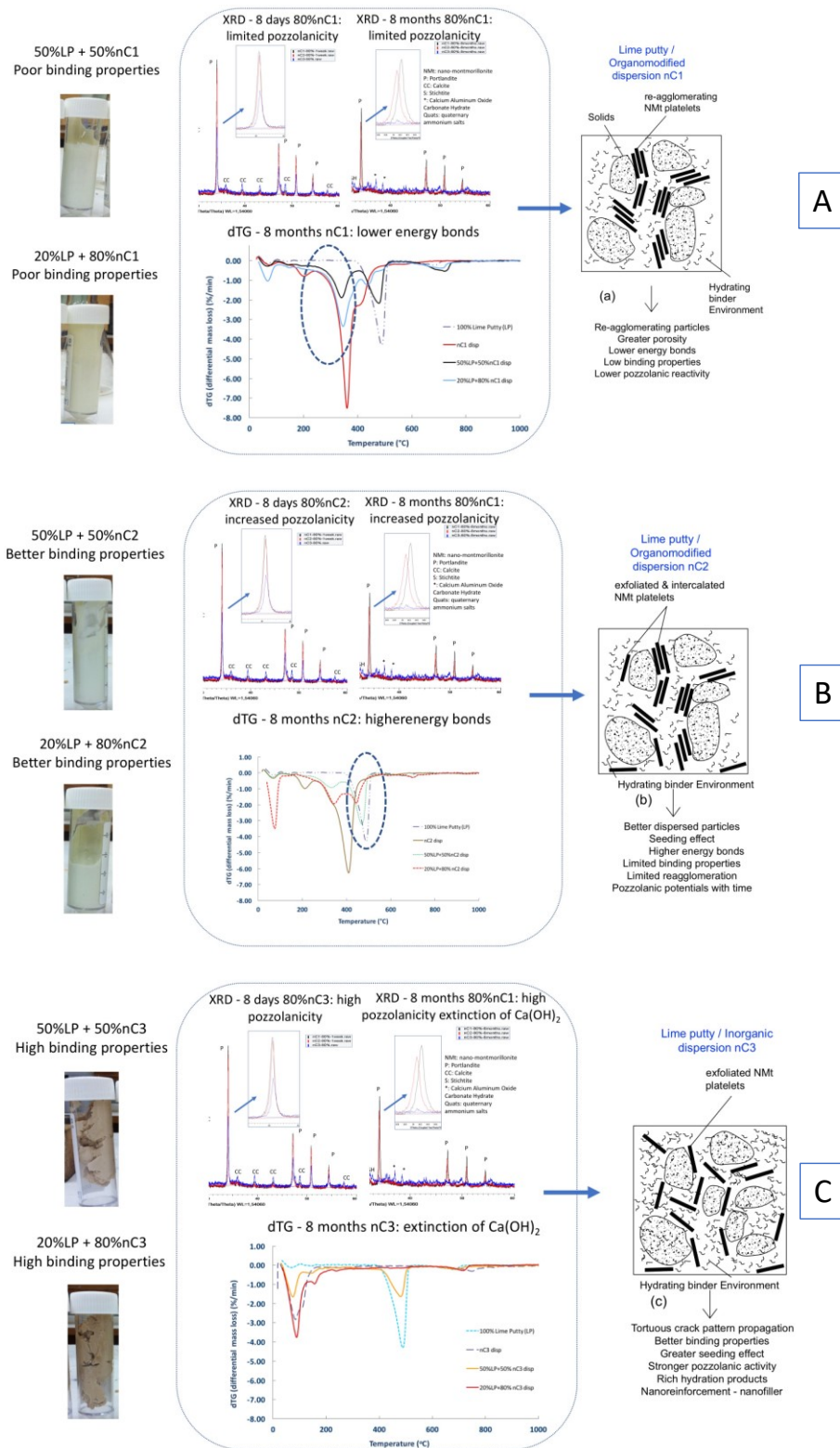
Lastly, the nanostructure of nC3 revealed exfoliated platelets, well dispersed in the volume of the paste acting as nanoreinforcement having potentials for seeding agent action. Better particle packing and increased platelets specific surface area was achieved in nC3, with NMt platelets playing the role of nanofillers. This configuration also allowed for significant inhibition of crack development, favouring flexural strength development and less brittle performance when added in binders.

In this research, these three different NMt dispersions were investigated in NMt/lime putty pastes with respect to their pozzolanic potentials. It can be claimed overall that the complex chemistry involved in the production of organomodified NMt dispersions affected not only their nanostructure as postulated by earlier studies [10] but also their pozzolanic performance. Adding to this, the type of surfactant or the amount of modifier present is setting a threshold on the allowable amount of NMt in lime putty or even cement pastes. In other words, it is possible that the organomodification process either due to the high amount of carbon present in the modifier or due to the alteration of the platelet surface charge, depending on the type of



686 surfactant used, is not allowing nC1 nanoplatelets and some of nC2 nanoplatelets to act as  
687 nucleation agents for reactions. The quaternary ammonium salts introduced in the galleries of  
688 the organomodified NMt as well as the surfactants employed for dispersing the platelets  
689 differentiate the chemical bond strength leading to lower energy formations for nC1 but  
690 maintaining the higher energy bonds found in the raw dispersions [10], in the NMt/lime patty  
691 pastes also for nC2 (Figure 8 (A) and(B)). This is the reason why the thermal gravimetric  
692 analyses of the LP/nC1 and LP/nC2 pastes differ, although the starting NMt powder was the  
693 same. nC1, which showed the poorest nanostructure, still exhibited some pozzolanic activity  
694 although this was challenged by the high amounts of carbon present in the sample and the re-  
695 agglomeration of the platelets. nC2, showed pozzolanic activity, increasing with curing age and  
696 higher proportions of nC2. nC3 exhibited the highest and most rapid consumption of  $\text{Ca(OH)}_2$   
697 towards production of calcium silicate and/or calcium aluminate hydrates possibly due to its  
698 simpler chemistry and nanostructure. The exfoliated platelets must have been individually  
699 reactive, engaging in pozzolanic reactions as seeding agents and catalysts (Figure 8 (C)).

700 Overall, the pozzolanic activity in terms of  $\text{Ca(OH)}_2$  consumption was more pronounced for the  
701 better dispersed NMt particles (nC2 and nC3). A qualitative interpretation of the TGA results  
702 shown is that both nC1 and particularly nC2 dispersions are forming new more thermally stable  
703 bonds in presence of  $\text{Ca(OH)}_2$  signalled by the new peaks at about  $435^\circ\text{C}$ . In fact, all LP/nC1  
704 and LP/nC2 pastes exhibit a two-stage decomposition with two distinct peaks at  $385^\circ\text{C}$  and at  
705  $435^\circ\text{C}$ , however the mass losses related to the peaks, shift depending on the NMt dispersion  
706 content. Therefore, the accuracy of the criterion could be challenged if the temperature range for  
707 the  $\text{Ca(OH)}_2$  consumption detection is broadened. However, the temperature range  $400\text{--}500^\circ\text{C}$   
708 selected for the criterion offers a good approximation. For this, it was postulated that inorganic  
709 NMt dispersions, show more distinct performance in terms of  $\text{Ca(OH)}_2$  consumption detection.



710

711 Figure 8: Binding properties, TGA and XRD related to nanostructure of (A) LP/ nC1, (B)

712 LP/ nC2 and (C) LP/ nC3 pastes

Furthermore, knowing that the average amorphous Si/Al ratio of nC1 is 4.23, nC2 is 4.08 and nC3 is 2.71 [10], all three dispersions can be expected to consume  $\text{Ca}(\text{OH})_2$  and form calcium silicate and/or calcium aluminate hydrates. Indeed, it can be argued that nC1 and nC3 produced more C–S–H, although it is acknowledged that molar calculations are difficult in this region due to the simultaneous decomposition of the modifier for nC1. Still, the carbonated hydrates traced in the 8-month-old LP/nC3 pastes reinforce this hypothesis.

These results presented herein are in agreement with results presented in NMt enhanced cement pastes. Extensive TG analyses on NMt enhanced cement pastes [8], suggest that blended cement pastes containing nC3 (ternary pastes of Portland cement, limestone and NMt) exhibited greater consumption of  $\text{Ca}(\text{OH})_2$  towards the production of additional C–S–H and ettringite, while nC1 and nC2 showed similar C–S–H and ettringite production until day 90.

It has been suggested the second derivate of thermogravimetric curve (DDTG) gives new possibilities for detailed investigations of overlapping decomposition mass losses [44], however the advanced mathematical elaboration involved [49] would only add to the already high level of inherent complexity and for this, such calculations were not considered in this research.

Further investigation of the LP/nC1 or LP/nC2 or LP/nC3 pastes would have provided visual representation of the pastes produced. For instance, scanning electron microscopy studies would have revealed agglomerated and hydrated particles. However, this was not considered necessary for the purpose of this paper, which was purely to devise a criterion by which the pozzolanic behaviour would be assessed in the complex matrix produced with the use of NMt. In fact, the already existing test methods, namely the Chapelle method, Fratinni method and Strength Activity Index have only been employed for the characterisation of calcined clays or cement pastes. The validity of the Chapelle method has been questioned for any other materials. Furthermore, due to the complex nature of the NMt dispersions, a new method should be

devised allowing for the quantification of the calcium hydroxide consumption. Although the mathematical elaboration of the results is not straightforward, still, the new method is offering more and in-depth information about the systems characterized. Lastly, given the assumptions made, the accuracy of the criterion was maintained.

The criterion of the new method was verified through a two-step process; (i) with respect to a theoretical estimation of the mass losses related to  $\text{Ca}(\text{OH})_2$  consumption and (ii) with respect to the net mass assigned to  $\text{Ca}(\text{OH})_2$  mathematically elaborated from the experimentally recorded value. It was also reinforced via XRD mineralogical analysis, as well as semi-quantitative analysis. Therefore, given the elemental composition of the NMt dispersions, TGA and XRD can be adequately combined to assess the pozzolanic behaviour of LP/nC1 or LP/nC2 or LP/nC3 pastes. The criterion was lastly validated via XRD analyses of the Chappelle products.

#### **4. Conclusions**

All things considered, primarily the nature (inorganic or organomodified) of NMt and the different dispersing agents both affect the thermal characteristics of NMt dispersions. For the first time, it was demonstrated that non-thermally treated Mt, nanomodified with the help of dispersion agents, can be potentially implemented in cementitious binders as a low carbon footprint, nanosized supplementary cementitious nanomaterial. Furthermore, a method for assessing the pozzolanic reactivity was devised, which allows for sound conclusions to be made, while simultaneously the Chappelle method was applied for the first time in (non-thermally treated) NMt dispersions. This research can provide a basis for the study of restoration pastes for superior properties. Therefore, the next generation of high performance materials produced via the manipulation of the size and distribution at the micro [47] and nano

level [48] is currently being studied and is expected to provide materials scientists and the engineering world with more sustainable options for the built environment.

To sum up, this study has:

- Devised a new criterion to assess the pozzolanic potential of NMt dispersions for use as supplementary cementitious materials through the study of NMt enhanced lime putty pastes.
- Applied Chapelle tests to (non-thermally treated) NMt dispersions for the first time, and results correlated well with the new method developed.
- Quantified the difference in pozzolanic reactivity of organomodified and inorganic NMt dispersions.
- Provided knowledge of the NMt surfactant decomposition stages and nanostructure that is essential for the interpretation of TG analysis of NMt enhanced lime putty pastes.
- Demonstrated that inorganic NMt dispersions exhibited rapid and pronounced pozzolanic activity signalling potential for advanced mechanical performance.
- Created a route for use of inorganic NMt dispersions in the production of lower carbon footprint cement binders as well as lime mortars for conservation of historic monuments.

## 5. Acknowledgements

The authors acknowledge the European Commission funding (FIBCEM project, grant Number 262954) and all partners are thanked for their input and for the supply of materials. The authors would also like to acknowledge the Department of Chemical Engineering at the University of Bath for the use of the TG analyser. Dr G.L. Pesce, University of Northumbria and. R.J. Ball,

University of Bath are thanked for scientific discussions. Moreover, the authors would like to thank the School of Chemical Engineering, at the Technical University of Athens (NTUA). Lastly, the authors acknowledge the Greek Ministry of Culture, Directorate of Restoration of Medieval and Post-Medieval Monuments, Department of Technical Research on Restoration for the use of the XRD software and for technical discussions.

## 6. References

- [1] H. Dalir, R.D. Farahani, V. Nhim, B. Samson, M. Levesque, D. Therriault, Preparation of highly exfoliated polyester-clay nanocomposites: process-property correlations, *Langmuir*. (2012).
- [2] R. Fernandez, F. Martirena, K.L. Scrivener, The origin of the pozzolanic activity of calcined clay minerals: A comparison between kaolinite, illite and montmorillonite, *Cem. Concr. Res.* 41 (2011) 113–122.  
doi:<http://dx.doi.org/10.1016/j.cemconres.2010.09.013>.
- [3] P.C. LeBaron, Z. Wang, T.J. Pinnavaia, Polymer-layered silicate nanocomposites: an overview, *Appl. Clay Sci.* 15 (1999) 11–29.
- [4] S. Papatzani, Effect of nanosilica and montmorillonite nanoclay particles on cement hydration and microstructure, *Mater. Sci. Technol.* 32 (2016) 138–153.  
doi:[10.1179/1743284715Y.00000000067](https://doi.org/10.1179/1743284715Y.00000000067).
- [5] L.B. De Paiva, A.R. Morales, F.R. Valenzuela Díaz, Organoclays: properties, preparation and applications, *Appl. Clay Sci.* 42 (2008) 8–24.
- [6] A. Vazquez, M. López, G. Kortaberria, L. Martín, I. Mondragon, Modification of montmorillonite with cationic surfactants. Thermal and chemical analysis

- 804 including CEC determination, *Appl. Clay Sci.* 41 (2008) 24–36.  
 805 doi:<http://dx.doi.org/10.1016/j.clay.2007.10.001>.
- 806 [7] C.B. Hedley, G. Yuan, B.K.G. Theng, Thermal analysis of montmorillonites  
 807 modified with quaternary phosphonium and ammonium surfactants, *Appl. Clay*  
 808 *Sci.* 35 (2007) 180–188. doi:<http://dx.doi.org/10.1016/j.clay.2006.09.005>.
- 809 [8] S. Papatzani, K. Paine, Dispersed Inorganic or Organommodified Montmorillonite  
 810 Clay Nanoparticles for Blended Portland Cement Pastes: Effects on Microstructure  
 811 and Strength, in: K. Sobolev, S.P. Shah (Eds.), *Nanotechnol. Constr. Proc.*  
 812 *NICOM5*, Springer International Publishing, 2015: pp. 131–139. doi:10.1007/978-  
 813 3-319-17088-6\_16.
- 814 [9] J. Calabria-Holley, S. Papatzani, B. Naden, J. Mitchels, K. Paine, Tailored  
 815 montmorillonite nanoparticles and their behaviour in the alkaline cement  
 816 environment, *Appl. Clay Sci.* 143 (2017) 67–75.  
 817 doi:<http://dx.doi.org/10.1016/j.clay.2017.03.005>.
- 818 [10] S. Papatzani, K. Paine, Inorganic and organommodified nano-montmorillonite  
 819 dispersions for use as supplementary cementitious materials - A novel theory based  
 820 on nanostructural studies, *Nanocomposites.* 3 (2017) 2–19.  
 821 doi:10.1080/20550324.2017.1315210.
- 822 [11] M. Fitos, E.G. Badogiannis, S.G. Tsivilis, M. Perraki, Pozzolanic activity of  
 823 thermally and mechanically treated kaolins of hydrothermal origin, *Appl. Clay Sci.*  
 824 116–117 (2015) 182–192. doi:<http://dx.doi.org/10.1016/j.clay.2015.08.028>.
- 825 [12] G. Kakali, T. Perraki, S. Tsivilis, E. Badogiannis, Thermal treatment of kaolin: the  
 826 effect of mineralogy on the pozzolanic activity, *Appl. Clay Sci.* 20 (2001) 73–80.  
 827 doi:[http://dx.doi.org/10.1016/S0169-1317\(01\)00040-0](http://dx.doi.org/10.1016/S0169-1317(01)00040-0).
- 828 [13] N. Farzadnia, A.A. Abang Ali, R. Demirboga, M.P. Anwar, Effect of halloysite

- 829 nanoclay on mechanical properties, thermal behavior and microstructure of cement  
830 mortars, *Cem. Concr. Res.* 48 (2013) 97–104.  
831 doi:<http://dx.doi.org/10.1016/j.cemconres.2013.03.005>.
- 832 [14] C. He, E. Makovicky, B. Osbaeck, Thermal treatment and pozzolanic activity of  
833 Na- and Ca-montmorillonite, *Appl. Clay Sci.* 10 (1996) 351–368.  
834 doi:[http://dx.doi.org/10.1016/0169-1317\(95\)00037-2](http://dx.doi.org/10.1016/0169-1317(95)00037-2).
- 835 [15] M. Aly, M.S.J. Hashmi, A.G. Olabi, M. Messeiry, A.I. Hussain, Effect of nano  
836 clay particles on mechanical, thermal and physical behaviours of waste-glass  
837 cement mortars, *Mater. Sci. Eng. A.* 528 (2011) 7991–7998.  
838 doi:[10.1016/j.msea.2011.07.058](http://dx.doi.org/10.1016/j.msea.2011.07.058).
- 839 [16] A. Hakamy, F.U.A. Shaikh, I.M. Low, Characteristics of nanoclay and calcined  
840 nanoclay-cement nanocomposites, *Compos. Part B Eng.* 78 (2015) 174–184.  
841 doi:<https://doi.org/10.1016/j.compositesb.2015.03.074>.
- 842 [17] A. Heath, K. Paine, S. Goodhew, M. Ramage, M. Lawrence, The potential for  
843 using geopolymers in concrete in the UK, *Proc. Inst. Civ. Eng. Constr. Mater.* 166  
844 (2013) 195–203.
- 845 [18] R. Kalpokaitė-Dičkuvienė, I. Lukošiušė, J. Čėsniienė, K. Brinkienė, A. Baltušnikas,  
846 Cement substitution by organoclay – The role of organoclay type, *Cem. Concr.*  
847 *Compos.* 62 (2015) 90–96. doi:[10.1016/j.cemconcomp.2015.04.021](http://dx.doi.org/10.1016/j.cemconcomp.2015.04.021).
- 848 [19] British Standards Institution, BS EN 459-1. Building lime. Definitions,  
849 specifications and conformity criteria, UK, 2015.
- 850 [20] J. Pontes, A. Santos Silva, P. Faria, Evaluation of Pozzolanic Reactivity of  
851 Artificial Pozzolans, *Mater. Sci. Forum.* 730–732 (2013) 433–438.  
852 doi:[10.4028/www.scientific.net/MSF.730-732.433](http://dx.doi.org/10.4028/www.scientific.net/MSF.730-732.433).
- 853 [21] R. Giorgi, M. Ambrosi, N. Toccafondi, P. Baglioni, Nanoparticles for Cultural



854 Heritage Conservation: Calcium and Barium Hydroxide Nanoparticles for Wall  
 855 Painting Consolidation, *Chem. – A Eur. J.* 16 (2010) 9374–9382.  
 856 doi:10.1002/chem.201001443.

857 [22] C. Rodriguez-Navarro, E. Ruiz-Agudo, M. Ortega-Huertas, E. Hansen,  
 858 Nanostructure and Irreversible Colloidal Behavior of Ca(OH)<sub>2</sub>: Implications in  
 859 Cultural Heritage Conservation, *Langmuir*. 21 (2005) 10948–10957.  
 860 doi:10.1021/la051338f.

861 [23] M. Margalha, A. Silva, M. do Rosário Veiga, J. de Brito, R. Ball, G. Allen,  
 862 Microstructural Changes of Lime Putty during Aging, *J. Mater. Civ. Eng.* 25  
 863 (2013) 1524–1532. doi:doi:10.1061/(ASCE)MT.1943-5533.0000687.

864 [24] A. Moropoulou, A. Bakolas, P. Moundoulas, E. Aggelakopoulou, S.  
 865 Anagnostopoulou, Strength development and lime reaction in mortars for repairing  
 866 historic masonries, *Cem. Concr. Compos.* 27 (2005) 289–294.  
 867 doi:http://dx.doi.org/10.1016/j.cemconcomp.2004.02.017.

868 [25] S. Papatzani, K. Paine, J. Calabria-Holley, A comprehensive review of the models  
 869 on the nanostructure of calcium silicate hydrates, *Constr. Build. Mater.* 74 (2015)  
 870 219–234. doi:http://dx.doi.org/10.1016/j.conbuildmat.2014.10.029.

871 [26] V. Morales-Florez, N. Findling, F. Brunet, Changes on the nanostructure of  
 872 cementitious calcium silicate hydrates (C–S–H) induced by aqueous carbonation, *J.*  
 873 *Mater. Sci.* 47 (2012) 764–771. doi:10.1007/s10853-011-5852-6.

874 [27] R. Largent, Estimation de l' activite pouzzolanique, *Bull. Liasons Lab. Pont*  
 875 *Chausees.* 93 (1978) 61–65.

876 [28] J.A. Kostuch, V. Walters, T.R. Jones, High performance concretes incorporating  
 877 metakaolin: a review, in: R.K. Dhir, M.R. Jones (Eds.), *Concr. 2000 Econ. Durable*  
 878 *Constr. Through Excell.*, E&FN SPON, London, 1996: pp. 1799–1811.

- 879 [29] V.S. Ramachandran, J.J. Beaudoin, Handbook of Analytical Techniques in  
880 Concrete Science and Technology, Principles, Techniques, and Applications,  
881 Noyes publications, New Jersey , 2001.
- 882 [30] Renishaw Plc, WiRE software, (2016). [http://www.renishaw.com/en/raman-](http://www.renishaw.com/en/raman-software-analysis--25909)  
883 [software-analysis--25909](http://www.renishaw.com/en/raman-software-analysis--25909) (accessed December 7, 2016).
- 884 [31] Bruker, EVA software, (2016). [https://www.bruker.com/products/x-ray-](https://www.bruker.com/products/x-ray-diffraction-and-elemental-analysis/x-ray-diffraction/xrd-software/eva/technical-details.html)  
885 [diffraction-and-elemental-analysis/x-ray-diffraction/xrd-software/eva/technical-](https://www.bruker.com/products/x-ray-diffraction-and-elemental-analysis/x-ray-diffraction/xrd-software/eva/technical-details.html)  
886 [details.html](https://www.bruker.com/products/x-ray-diffraction-and-elemental-analysis/x-ray-diffraction/xrd-software/eva/technical-details.html) (accessed December 7, 2017).
- 887 [32] S. Papatzani, K. Paine, Polycarboxylate / nanosilica modified quaternary cement  
888 formulations - enhancements and limitations - in press, Adv. Cem. Res. (2017).  
889 doi:<https://doi.org/10.1680/jadcr.17.00111>.
- 890 [33] E.T. Carlson, H.A. Berman, Some observations on the calcium aluminate  
891 carbonate hydrates, J. Res. Natl. Bur. Stand. (1934). 64 (1960) 333–341.
- 892 [34] R. Snellings, A. Salze, K.L. Scrivener, Use of X-ray diffraction to quantify  
893 amorphous supplementary cementitious materials in anhydrous and hydrated  
894 blended cements, Cem. Concr. Res. 64 (2014) 89–98.  
895 doi:<http://dx.doi.org/10.1016/j.cemconres.2014.06.011>.
- 896 [35] S. Papatzani, Nanotechnologically modified cements: Effects on hydration,  
897 microstructure and physical properties, University of Bath, 2014.
- 898 [36] W. Xie, Z. Gao, K. Liu, W.-P. Pan, R. Vaia, D. Hunter, et al., Thermal  
899 characterization of organically modified montmorillonite, Thermochim. Acta. 367–  
900 368 (2001) 339–350. doi:[http://dx.doi.org/10.1016/S0040-6031\(00\)00690-0](http://dx.doi.org/10.1016/S0040-6031(00)00690-0).
- 901 [37] Q. Zhou, R.L. Frost, H. He, Y. Xi, Changes in the surfaces of adsorbed para-  
902 nitrophenol on {HDTMA} organoclay—The {XRD} and {TG} study, J. Colloid  
903 Interface Sci. 307 (2007) 50–55. doi:<http://dx.doi.org/10.1016/j.jcis.2006.11.016>.

- 904 [38] R.J. Ball, G.L.A. Pesce, C.R. Bowen, G.C. Allen, Characterisation of  
 905 Lime/Metakaolin Paste Using Impedance Spectroscopy, *Key Eng. Mater.* 517  
 906 (2012) 487–494. doi:10.4028/www.scientific.net/KEM.517.487.
- 907 [39] G.L. Pesce, C.R. Bowen, J. Rocha, M. Sardo, G.C. Allen, P.J. Walker, et al.,  
 908 Monitoring hydration in lime-metakaolin composites using electrochemical  
 909 impedance spectroscopy and nuclear magnetic resonance spectroscopy, *Clay*  
 910 *Miner.* 49 (2014) 341–358. doi:10.1180/claymin.2014.049.3.01.
- 911 [40] L. Vieille, I. Rousselot, F. Leroux, J.-P. Besse, C. Taviot-Guého, Hydrocalumite  
 912 and Its Polymer Derivatives. 1. Reversible Thermal Behavior of Friedel’s Salt: A  
 913 Direct Observation by Means of High-Temperature in Situ Powder X-ray  
 914 Diffraction, *Chem. Mater.* 15 (2003) 4361–4368. doi:10.1021/cm031069j.
- 915 [41] S.J. Mills, A.G. Christy, J.-M. Génin, T. Kameda, F. Colombo, Nomenclature of  
 916 the hydrotalcite supergroup: natural layered double hydroxides, *Mineral. Mag.* 76  
 917 (2012) 1289–1336.
- 918 [42] J. Bouzaid, R.L. Frost, Thermal decomposition of stichtite, *J. Therm. Anal.*  
 919 *Calorim.* 89 (2007) 133–135. doi:10.1007/s10973-005-7272-9.
- 920 [43] A. V Borhade, A.G. Dholi, D.R. Tope, S.G. Wakchaure, Solvothermal synthesis  
 921 and crystal structure of aluminogermanate halide sodalites using organic solvent,  
 922 *Indian J. Pure Appl. Phys.* 50 (2012) 576–582.
- 923 [44] M. Földvári, Handbook of the thermogravimetric system of minerals and its use in  
 924 geological practice, 2011. doi:10.1556/CEuGeol.56.2013.4.6.
- 925 [45] K. Byrappa, M.K. Devaraju, P. Madhusudan, A.S. Dayananda, B.V.S. Kumar,  
 926 H.N. Girish, et al., Synthesis and characterization of calcium aluminum silicate  
 927 hydroxide (CASH) mineral, *J. Mater. Sci.* 41 (2006) 1395–1398.  
 928 doi:10.1007/s10853-006-7413-y.

- 929 [46] S. Goñi, A. Guerrero, M.P. Luxán, A. Macías, Activation of the fly ash pozzolanic  
930 reaction by hydrothermal conditions, *Cem. Concr. Res.* 33 (2003) 1399–1405.  
931 doi:[http://dx.doi.org/10.1016/S0008-8846\(03\)00085-1](http://dx.doi.org/10.1016/S0008-8846(03)00085-1).
- 932 [47] A. Gameiro, A. Santos Silva, P. Faria, J. Grilo, T. Branco, R. Veiga, et al.,  
933 Physical and chemical assessment of lime–metakaolin mortars: Influence of  
934 binder:aggregate ratio, *Cem. Concr. Compos.* 45 (2014) 264–271.  
935 doi:<http://dx.doi.org/10.1016/j.cemconcomp.2013.06.010>.
- 936 [48] S. Goñi, A. Guerrero, Accelerated carbonation of Friedel’s salt in calcium  
937 aluminate cement paste, *Cem. Concr. Res.* 33 (2003) 21–26.  
938 doi:[http://dx.doi.org/10.1016/S0008-8846\(02\)00910-9](http://dx.doi.org/10.1016/S0008-8846(02)00910-9).
- 939 [49] T. Székely, G. Várhegyi, F. Till, The determination and use of the second  
940 derivative thermogravimetric function (DDTG) and the calculation of the kinetic  
941 constants of some decomposition reaction types, *J. Therm. Anal.* 5 (1973) 227–  
942 237. doi:[10.1007/BF01950371](https://doi.org/10.1007/BF01950371).
- 943
- 944

## 945 7. Appendix – Decomposition mass loss calculations

### 946 8 days – experimental mass loss calculations

947 The following can be noted with respect to the results presented in Table 5 [equation 1 –  
948  $M_{CH}$  calculation].

949 For the mass loss observed within 400-500°C for 50%LP+50%nC:

950  $M_{CH}^{nC1} = 13.97\% - 9.48\% \times 50\% = \boxed{9.2\%}$  [9.48% corresponds to the mass loss of nC1 within  
951 400-500°C (Table 3)].

952  $M_{CH}^{nC2} = 18.63\% - 20.14\% \times 50\% = \boxed{8.6\%}$  [20.14% corresponds to the mass loss of nC2 within  
953 400-500°C (Table 3)].

954 It is interesting to note that:  $10.53 + 13.97 = 24.5\% \sim 50\% \times 44.8\% = 22.4\%$  [precisely 50%  
955 nC1 decomposition mass loss (Table 3)] and

956  $7.35 + 18.63 = 25.98\% \sim 50\% \times 46\% = 23\%$  [precisely 50% nC2 decomposition mass loss  
957 (Table 3)]

958  $M_{CH}^{nC3} = 8.88\% - 1.0\% \times 50\% = \boxed{8.4\%}$  [1.0% corresponds to the mass loss of nC3 within 400-  
959 500°C (Table 4)].

960 For the mass loss observed within 400-500°C for 20%LP+80%nC:

961  $M_{CH}^{nC1} = 12.72\% - 9.48\% \times 80\% = \boxed{5.14\%}$ , therefore significant reduction in  $Ca(OH)_2$  was  
962 achieved by **80% nC1**.

963  $M_{CH}^{nC2} = 16.11\% - 20.14\% \times 80\% = \boxed{0.0\%}$ , therefore significant reduction in  $Ca(OH)_2$  was  
 964 achieved by **80% nC2**.

965  $M_{CH}^{nC3} = 3.6\% - 1.0\% \times 80\% = \boxed{2.8\%}$ , therefore significant reduction of  $Ca(OH)_2$  was achieved  
 966 by **80% nC3**.

967 **Calculation of decomposition of calcium carbonate [equation 2 –  $M_{CC}$  calculation]**

968  $M_{CC} = M_{loss}^{600-800} - M_{NMt}^{600-800} \times (\%NMt)$

969 For 50% nC1:  $M_{CC} = 5.93\% - 0 \times 50\% = 5.9\%$

970 For 50% nC2:  $M_{CC} = 4.19\% - 0 \times 50\% = 4.2\%$

971 For 50% nC3:  $M_{CC} = 11.73\% - 4.4 \times 50\% = 9.5\%$

972 For 80% nC1:  $M_{CC} = 11.3\% - 0 \times 80\% = 11.3\%$

973 For 80% nC2:  $M_{CC} = 4.64\% - 0 \times 80\% = 6.46\%$

974 For 80% nC3:  $M_{CC} = 9\% - 4.4 \times 80\% = 5.5\%$

975 Table Ap-1: Elaboration of experimental results at day 8

Experimental values						
Sample	$M_{CH}$ (%)	$M_{CC}$ (%)	$MM_{CH}$	$MM_{CC}$	$MM_{carbCH}$	$MM_{totCH}$
	Eq1	Eq2	Eq3	Eq4		Eq5
<b>50%LP+50%nC1</b>	9.20	5.93	37.86	13.48	9.99	47.85
<b>50%LP+50%nC2</b>	8.60	4.19	35.39	9.52	7.05	42.44
<b>50%LP+50%nC3</b>	8.40	9.50	34.57	21.59	15.99	50.56
<b>20%LP+80%nC1</b>	5.15	11.30	21.15	25.68	19.02	40.17

20%LP+80%nC2	0.00	6.46	0.00	14.77	10.94	10.94
20%LP+80%nC3	2.80	5.50	11.52	12.50	9.26	20.78

976

## 977 **8 days – theoretical mass loss calculations**

978 Estimation of theoretical mass loss attributed to CH:

979 Furthermore, theoretically, if nC1/2/3 and LP were not engaged in reactions, disregarding  
980 carbonation, according to the mass losses recorded in Table 2 to 5 **between 400-500°C** for:

981 50% LP+50% nC1 the mass loss should have been  $50\% \times 20.20 + 50\% \times 9.48 = 14.8\% > 13.97$

982 50% LP+50% nC2 the mass loss should be  $50\% \times 20.20 + 50\% \times 20.14 = 20.2\% > 18.63$

983 50% LP+50% nC3 the mass loss should be  $50\% \times 20.20 + 50\% \times (1) = 10.6\% > 8.88$

984 20% LP+80% nC1 the mass loss should be  $20\% \times 20.20 + 80\% \times 9.48 = 11.6\% < 12.72$

985 20% LP+80% nC2 the mass loss should be  $20\% \times 20.20 + 80\% \times 20.14 = 20.0\% > 16.11$

986 20% LP+80% nC3 the mass loss should be  $20\% \times 20.20 + 80\% \times 1 = 4.8\% > 3.6$

987

988 Estimation of theoretical mass loss attributed to the **decomposition of calcium carbonate**

989 **[equation 2 – M<sub>CC</sub> calculation]:**

$$990 \quad M_{CC} = M_{loss}^{600-800} - M_{NMt}^{600-800} \times (\%NMt)$$

991 For 50% nC3:  $M_{CC} = 3.52 \times 50\% + 4.4 \times 50\% = 4\%$

992 For 80% nC3:  $M_{CC} = 3.52 \times 20\% + 4.4 \times 80\% = 4.2\%$

993

994 Table Ap-2: Elaboration of theoretical values at day 8

Theoretical values						
Sample	M <sub>CH</sub>	M <sub>CC</sub>	MM <sub>CH</sub>	MM <sub>CC</sub>	MM <sub>carbCH</sub>	MM <sub>totCH</sub>
	(%)	(%)				
	Eq1	Eq2	Eq3	Eq4		Eq5
50%LP+50%nC1	14.80	0.00	60.91	0.00	0.00	60.91
50%LP+50%nC2	20.20	0.00	83.13	0.00	0.00	83.13
50%LP+50%nC3	10.60	4.00	43.62	9.10	6.70	50.32
20%LP+80%nC1	11.60	0.00	47.74	0.00	0.00	47.74
20%LP+80%nC2	20.00	0.00	82.30	0.00	0.00	82.30
20%LP+80%nC3	4.80	4.20	19.75	9.50	7.00	26.75

995

## 996 **8 months – experimental mass loss calculations**

997 The following can be noted with respect to the results presented in Table 7 [equations 1  
998 and 2].

999 1: At 100% LP, the mass loss related to Ca(OH)<sub>2</sub> was 21.24%, therefore for 50% LP it would be  
1000 10.6% and for 20% LP, the mass loss would be 4.2%.

1001 2: for the mass loss observed within 400-500°C: 12.47% – 9.48% $\times$ 50% = 7.73% < 10.6%,  
1002 hence some reduction of Ca(OH)<sub>2</sub> was achieved by 50% nC1.

1003 3: for the mass loss observed within 400-500°C: 17.26% – 20.14% $\times$ 50% = 7.19% < 10.6%,  
1004 therefore significant reduction of Ca(OH)<sub>2</sub> was achieved by 50% nC2.

1005 Moreover, it is interesting to add the two underlined mass losses:



1006 2A:  $10.93 + 12.47 = 23.4\% \sim 50\% \times 44.8\% = 22.4\%$  (50% nC1 decomposition mass loss),  
1007 therefore, yielding absolute accuracy.

1008 3A:  $6.9 + 17.26 = 24.16\% \sim 50\% \times 46.09\% = 23.5\%$  (50% nC2 decomposition mass loss),  
1009 therefore, yielding absolute accuracy.

1010 4: For the mass loss observed within 400-500°C:  $9.23\% - 1.0\% \times 50\% = 8.73\% < 10.6\%$ ,  
1011 therefore significant reduction of  $\text{Ca(OH)}_2$  was achieved by 50% nC3.

1012 5: For the mass loss observed within 400-500°C:  $8.1\% - 9.48\% \times 80\% = 0.52\% < 4.2\%$ , therefore  
1013 almost elimination of  $\text{Ca(OH)}_2$  was achieved by 80% nC1.

1014 6: For the mass loss observed within 400-500°C:  $11.37\% - 20.14\% \times 80\% = 0\% < 4.2\%$ ,  
1015 therefore elimination of  $\text{Ca(OH)}_2$  was achieved by 80% nC2.

1016 7: For the mass loss observed within 400-500°C:  $1.42\% - 1.0\% \times 80\% = 0.62\% < 4.2\%$ ,  
1017 therefore almost elimination of  $\text{Ca(OH)}_2$  was achieved by 80% nC3.

1018

## 1019 **Calculation of decomposition of calcium carbonate [equation 2]**

1020 
$$M_{CC} = M_{\text{loss}}^{600-800} - M_{\text{NMt}}^{600-800} \times (\% \text{NMt})$$

1021 For 50% nC1:  $M_{CC} = 5.57\% - 0 \times 50\% = 5.6\%$

1022 For 50% nC2:  $M_{CC} = 3.4\% - 0 \times 50\% = 3.4\%$

1023 For 50% nC3:  $M_{CC} = 2.94\% - 4.4 \times 50\% = 0.7\%$

1024 For 80% nC1:  $M_{CC} = 5.5\% - 0 \times 80\% = 5.5\%$

1025 For 80% nC2:  $M_{CC} = 4.93\% - 0 \times 80\% = 4.9\%$

1026 For 80% nC3:  $M_{CC} = 3\% - 4.4 \times 80\% = 0.0\%$

1027 Table Ap-3: Elaboration of experimental values at month 8

Experimental values						
Sample	$M_{CH}$	$M_{CC}$	$MM_{CH}$	$MM_{CC}$	$MM_{carbCH}$	$MM_{totCH}$
	Eq1	Eq2	Eq3	Eq4		Eq5
50%LP+50%nC1	7.73	5.57	31.81	12.66	9.37	41.18
50%LP+50%nC2	7.19	3.40	29.59	7.73	5.72	35.31
50%LP+50%nC3	8.73	0.73	35.93	1.66	1.23	37.16
20%LP+80%nC1	0.52	5.50	2.14	12.50	9.25	11.39
20%LP+80%nC2	0.00	4.93	0.00	11.20	8.29	8.29
20%LP+80%nC3	0.62	0.00	2.55	0.00	0.00	2.55

1028

1029

### 1030 **8 months – theoretical mass loss calculations**

1031 Disregarding carbonation, theoretically, according to the mass losses recorded in Table 2 to 4

1032 and Table 7 between **400-500°C** for:

1033 50% LP+50% nC1 the mass loss should be  $50\% \times (21.24) + 50\% \times 9.48 = 15.4\%$  > 12.47

1034 50% LP+50% nC2 the mass loss should be  $50\% \times 21.24 + 50\% \times 20.14 = 20.7\%$  > 17.26

1035 50% LP+50% nC3 the mass loss should be  $50\% \times 21.24 + 50\% \times 1 = 11.1\%$  > 9.23

1036 20% LP+80% nC1 the mass loss should be  $20\% \times 21.24 + 80\% \times 9.48 = 11.8\%$  > 8.10

1037 20% LP+80% nC2 the mass loss should be  $20\% \times 21.24 + 80\% \times 20.14 = 20.4\%$  > 11.37

1038 20% LP+80% nC3 the mass loss should be  $20\% \times 21.24 + 80\% \times 1 = 5.0\%$  > 1.4

1039 Estimation of theoretical mass loss attributed to the **decomposition of calcium carbonate**

1040 **[equation 2 – M<sub>CC</sub> calculation]:**

1041 
$$M_{CC} = M_{loss}^{600-800} - M_{NMt}^{600-800} \times (\%NMt)$$

1042 For 50% nC3:  $M_{CC} = 3.52 \times 50\% + 4.4 \times 50\% = 4\%$

1043 For 80% nC3:  $M_{CC} = 3.52 \times 20\% + 4.4 \times 80\% = 4.2\%$

1044 Table Ap-4: Elaboration of theoretical values at month 8

Theoretical values						
Sample	M <sub>CH</sub>	M <sub>CC</sub>	MM <sub>CH</sub>	MM <sub>CC</sub>	MM <sub>carbCH</sub>	MM <sub>totCH</sub>
	(%)	(%)				
	Eq1	Eq2	Eq3	Eq4		Eq5
50%LP+50%nC1	15.40	0.00	63.37	0.00	0.00	63.37
50%LP+50%nC2	20.70	0.00	85.19	0.00	0.00	85.19
50%LP+50%nC3	11.10	4.00	45.68	9.10	6.70	52.41
20%LP+80%nC1	11.80	0.00	48.56	0.00	0.00	48.56
20%LP+80%nC2	20.40	0.00	83.95	0.00	0.00	83.25
20%LP+80%nC3	5.00	4.20	20.58	9.50	7.00	27.65

1045